Dependence on extracellular Ca^{2+}/K^+ antagonism of inspiratory centre rhythms in slices and *en bloc* preparations of newborn rat brainstem

Araya Ruangkittisakul, Lucia Secchia, Troy D. Bornes, Darren M. Palathinkal and Klaus Ballanyi

Department of Physiology and Perinatal Research Centre, University of Alberta, Edmonton, Alberta, Canada T6G 2S2

The pre-Bötzinger Complex (preBötC) inspiratory centre remains active in isolated brainstem–spinal cords and brainstem slices. The extent to which findings in these models depend on their dimensions or superfusate $[K^+]$ and $[Ca^{2+}]$ (both of which determine neuronal excitability) is not clear. We report here that inspiratory-related rhythms in newborn rat slices and brainstem–spinal cords with defined boundaries were basically similar in physiological Ca^{2+} (1.2 mM) and K^+ (3 mM). Hypoglossal nerve rhythm was 1 : 1-coupled to preBötC activity in slices and to cervical nerve bursts in *en bloc* preparations lacking the facial motonucleus (VII). Hypoglossal rhythm was depressed in brainstems containing (portions of) VII, while pre/postinspiratory lumbar nerve bursting was present only in preparations with $>$ 79% VII. preBötC-related slice rhythms were inhibited in 1.5 mM Ca^{2+} solution, whereas their longevity and burst rate were substantially augmented in 1 mM Ca^{2+}. Ca^{2+} depression of slice rhythms was antagonized by raising superfusate K^+ to 8–10 mM. This strong extracellular Ca^{2+}/K^+ antagonism of inspiratory (motor) rhythms was also revealed in brainstem–spinal cords without VII, while the inhibition was progressively attenuated with increasing amount of rostral tissue. We hypothesize that depression of hypoglossal rhythm and decreased Ca^{2+} sensitivity of preBötC rhythm are probably not related to an increased content of rostral respiratory structures, but rather to larger brainstem dimensions resulting in interstitial gradients for neuromodulator(s) and K^+, respectively. We discuss whether block of pre/postinspiratory activity in preparations with $<$ 79% VII is due to impairment of the pathway from preinspiratory interneurons to abdominal muscles

(Resubmitted 9 August 2007; accepted after revision 18 August 2007; first published online 23 August 2007)
Corresponding author K. Ballanyi: Department of Physiology and Perinatal Research Centre, 220 HMRC, University of Alberta, Edmonton, Alberta, Canada T6G 2S2. Email: klaus.ballanyi@ualberta.ca

The neural control of breathing is studied in reduced preparations such as isolated newborn rat brainstem–spinal cords (Smith *et al.* 1990; Ballanyi *et al.* 1999). Microsectioning of this *in vitro* model showed that neurons of the pre-Bötzinger Complex (preBötC) inspiratory centre remain active in a transverse brainstem slice (Smith *et al.* 1991). In both, slice and *en bloc* models, rhythmogenic preBötC networks and preBötC-driven motor circuits are studied under quite divergent experimental conditions. preBötC slice thickness ranges from 200 to 1000 μm, and rostrocaudal boundaries of slices and brainstem–spinal cords vary notably (Rekling *et al.* 1996; Ballanyi *et al.* 1999; Koshiya & Smith, 1999; Ruangkittisakul *et al.* 2006). This may affect fictive inspiratory rhythms as the preBötC is neighboured by other ventral respiratory column structures such as the more rostral Bötzinger complex (BötC) and the parafacial respiratory group (pFRG), which is presumably closely associated with the retrotrapezoid nucleus (RTN) (Monnier *et al.* 2003; Feldman & Del Negro, 2006). While differences in the content of ventral respiratory column structures may modulate preBötC rhythms specifically, unspecific modulation may arise from interstitial accumulation or, conversely, washout of neuromodulator(s), which both depend on physical dimensions of isolated preparations (Ballanyi, 1999; Ruangkittisakul *et al.* 2006). preBötC activity may also be affected by superfusate constituents such as Ca^{2+} and K^+ that modulate excitability in other neuronal systems (Hille, 2001; Somjen, 2002). The most common values of interstitial $[Ca^{2+}]$ and $[K^+]$ in diverse mammalian brain regions *in vivo* are 1.2 mM and 3 mM, respectively (Somjen, 2002). This contrasts with a wide range of

A. Ruangkittisakul and L. Secchia contributed equally to this work.

 DOI: 10.1113/jphysiol.2007.142760

superfusate Ca^{2+} (0.8–2.4 mM) and K^+ (3–11 mM) in studies on isolated respiratory networks (Suzue, 1984; Smith *et al.* 1991; Johnson *et al.* 1996; Rekling *et al.* 1996; Ruangkittisakul *et al.* 2006).

Differences in dimensions of preparations and/or superfusate composition may be responsible for discrepant findings, e.g. regarding the capability of the isolated preBötC to generate rhythm. The above transection study (Smith *et al.* 1991) showed that the rate of inspiratory-related cervical nerve bursting is not affected by transection between preBötC and facial motonucleus (VII) in 1.5 mM Ca^{2+} solution. Other studies on this model showed that such transection depressed inspiratory burst rate in 2 mM Ca^{2+} (McLean & Remmers, 1994), whereas cervical rhythm was abolished following transection in 'Suzue-type' solution with 2.4 mM Ca^{2+} (Onimaru & Homma, 1987). We hypothesize that effects of brainstem transection on inspiratory-related rhythms depend critically on superfusate Ca^{2+}.

The constancy of extensions of respiratory brainstem marker nuclei in early postnatal rats enables 'online' histology for generation of preBötC slices with defined boundaries that are capable of stable rhythm in 3 mM K^+ (Ruangkittisakul *et al.* 2006). Our finding here that cranial nerves and blood vessels are ventral brainstem surface landmarks with a constant anatomical relation to the marker nuclei allowed generation of brainstem–spinal cords with defined rostral boundary. As one major aim of our study, we quantified in these *en bloc* preparations in physiological (1.2/3 mM) Ca^{2+}/K^+ the relation of their boundaries to the rate and duration of inspiratory cervical/hypoglossal nerve bursts and longevity of these rhythms, and compared the findings with those in the above slices. We then studied the Ca^{2+} dependence of preBötC (related) rhythms in both models. Finally, we elucidated the dependence on the rostral brainstem boundary of pre/postinspiratory lumbar nerve activity driving expiratory muscles (Janczewski *et al.* 2002; Janczewski & Feldman, 2006).

We found that preBötC (related) rhythms in 1.2 mM Ca^{2+} and 3 mM K^+ were basically similar in slices and *en bloc* preparations. Hypoglossal rhythm was stable and 1 : 1-coupled to preBötC population activity in slices and to cervical bursting in brainstems without VII. In contrast, hypoglossal rhythm was depressed in *en bloc* preparations with more rostral boundaries, while pre/postinspiratory lumbar nerve bursting was only present in brainstems with a major portion of VII. Most importantly, preBötC bursting and associated motor rhythms in slices and *en bloc* medullas without VII were greatly depressed upon Ca^{2+} elevation by only 0.5 and 0.6 mM, respectively, and were reactivated by 8–10 mM K^+. Conversely, in 1 mM instead of 1.2 mM Ca^{2+} solution, slice rhythms had a substantially greater longevity (> 3.5 h *vs.* ∼1.5 h) and higher long-term burst rate. After spontaneous arrest of rhythm in 3 mM K^+ and 1–1.2 mM Ca^{2+} in (slice) preparations with exposed preBötC, similar rhythm was reevoked by 6–7 mM K^+ and cAMP elevation by rolipram.

We discuss whether lack of pre/postinspiratory activity in preparations with < 79% VII is due to impairment of the pathway from preinspiratory (pFRG) interneurons to abdominal expiratory muscles. We hypothesize that depression of hypoglossal rhythm and attenuated Ca^{2+} sensitivity of preBötC rhythm in less-reduced *en bloc* medullas is probably not related to increased content of rostral respiratory structures, but rather due to larger dimensions creating interstitial gradients for inhibitory neuromodulator(s) and K^+. The strong dependence of inspiratory rhythms on an extracellular Ca^{2+}/K^+ antagonism suggests use of 1 mM Ca^{2+} for analysing isolated preBötC functions in 3 mM K^+.

Methods

Ethical approval

The University of Alberta Animal Care and Ethics Committee approved all procedures and provided governance for the animal care.

Preparations and solutions

Brainstem–spinal cord preparations were generated from 57 Sprague–Dawley (SD) and 54 Wistar (W) rats between postnatal day 0 (P0) and P4. Animals were anaesthetized with 2–3% isoflurane and rapidly decerebrated after the paw withdrawal reflex disappeared. The neuraxis was isolated at 19–22°C in superfusate (for composition, see below) (Brockhaus & Ballanyi, 1998, 2000). The brainstem was transected rostral to the trigeminal nerve (Fig. 1), and the spinal cord cut at the cervical level ($C_{6\text{-}8}$), except for one series of experiments in which the entire spinal cord was isolated for recording from ventral lumbar ($L_{1\text{-}2}$) nerve roots. To obtain preparations with a defined boundary, rostral brainstem tissue including the pons was manually sectioned with a razor blade based on the constancy of ventral surface anatomical landmarks that we have revealed here (Fig. 1; see also online supplemental material Fig. S1). The desired rostrocaudal sectioning level was histologically verified after the electrophysiological experiments (supplemental Figs S1–S3). Preparations were fixed with the ventral side up at the spinal cord to the bottom silicone layer of the superfusion chamber with insect pins (volume 1.5 ml). Further stabilization was achieved by suction electrodes used to record nerve activities (see below). Superfusate was administered at a flow rate of 5 ml min^{-1} via a peristaltic pump (Watson-Marlow Alitea-AB, Sin-Can, Calgary, Alberta, Canada). Temperature in the recording chamber was kept at 25–27°C (TC-324B, Harvard Apparatus, Saint-Laurent, Quebec, Canada).

Superfusate with $[Ca^{2+}]$ (Heinemann *et al.* 1977; Nicholson *et al.* 1978; Hansen, 1985; Richter & Acker, 1989; Trippenbach *et al.* 1990; Nilsson *et al.* 1993; Puka-Sundvall *et al.* 1994; Somjen, 2002; Brown *et al.* 2004) and $[K^+]$ (Leusen, 1972; Hansen, 1985; Somjen, 2002; Brown *et al.* 2004) resembling most common values in the extracellular space of brain tissue *in vivo*, i.e. 1.2 mM and 3 mM, respectively, contained (mM): 120 NaCl, 3 KCl, 1.2 $CaCl_2$, 1 $MgCl_2$, 1.25 NaH_2PO_4, 26 $NaHCO_3$ and 30 D-glucose (pH adjusted to 7.4 by gassing with 95% O_2, 5% CO_2).

preBötC-related rhythms in brainstem–spinal cords in standard solution were compared with those in solution of elevated Ca^{2+}, K^+ and Mg^{2+} (2.4, 6.2 and 1.3 mM, respectively), very similar to that in the first study (Suzue, 1984) and numerous follow-up reports on this and other isolated respiratory networks (e.g. Oshima *et al.* 2000; Herlenius *et al.* 2002; Iizuka, 2004; St. John *et al.* 2005; Kuwana *et al.* 2006; Onimaru *et al.* 2006). This 'Suzue-type' solution contained (mM): 120 NaCl, 6.2 KCl, 2.4 $CaCl_2$, 1.3 $MgCl_2$, 1.25 NaH_2PO_4, 26 $NaHCO_3$ and 30 D-glucose (pH adjusted to 7.4 by gassing with 95% O_2, 5% CO_2). In a related series of experiments, Ca^{2+} and K^+ in the standard solution were varied between 1.2 and 6 mM, and 3 and 10 mM, respectively.

preBötC-related rhythms were also studied in 600 μm thick 'm-preBötC slices' with the preBötC in the middle (Ruangkittisakul *et al.* 2006). After removal of the cerebellum and sectioning close to the caudal cerebellar artery (De Araujo & Campos, 2005) (Fig. 1), the brainstem of P0–4 SD ($n = 8$) or W rats ($n = 28$) was glued rostral side down to a metal plate and transferred to a vibrating microtome (Leica VT1000S, Leica Microsystems, Richmond Hill, Ontario, Canada). Serial transverse sectioning (100 μm) was stopped, and one 'rhythmic' slice was cut, when specific landmarks were reached, in particular subregions of the inferior olive (Fig. 1 and supplemental Fig. S1). Slices were fixed caudal side up with insect pins in the recording chamber and superfused with standard saline in which Ca^{2+} and K^+ were varied between 1 and 1.8 mM and 3 and 10 mM, respectively, at either 1 or 2 mM Mg^{2+} (Ruangkittisakul *et al.* 2006).

Rolipram (Sigma-Aldrich, Canada), a phosphodiesterase-4 blocker (O'Donnell & Zhang, 2004) stimulating inspiratory rhythm (Ruangkittisakul & Ballanyi, 2006; Ruangkittisakul *et al.* 2006), was kept frozen in stock solution (1 mM in dimethyl sulfoxide). Chemicals for salines were purchased from Fisher Scientific (Oakville, Ottawa, Ontario, Canada).

Electrophysiological recording

Discharge of preBötC-driven motoneurons providing inspiratory motor output in brainstem–spinal cord preparations (Smith *et al.* 1990; Ballanyi *et al.* 1999) was recorded from ventral spinal ($C_{3–4}$) and cranial (hypoglossal) nerve roots with suction electrodes (outer diameter 80–250 μm) filled with standard superfusate. In brainstem preparations with a complete spinal cord, activity was recorded simultaneously from $C_{3–4}$ and ventral $L_{1\text{-}2}$ roots, the latter containing axons of pre/postinspiratory active motoneurons that appear to be driven by the pFRG and innervate expiratory abdominal muscles (Janczewski *et al.* 2002; Iizuka, 2004). Neuronal population activity was recorded with a differential amplifier ($\times$10 000, DAM 50, World Precision Instruments, Sarasota, FL, USA), bandpass-filtered (0.3–3 kHz) and integrated. In the slices, suction electrode recording was done at the caudal surface from the ventral respiratory column containing the preBötC (Alheid *et al.* 2004), in most cases combined with recording from one hypoglossal nerve root. Signals were fed into a computer (sampling rate 1 kHz) via a digital recording system (Powerlab/8SP, ADInstruments, Colorado Springs, CO, USA).

Data analysis

Respiratory-related activity of brainstem–spinal cord preparations and slices was continuously recorded and quantified by measuring every 20 min over 2 min time periods the frequency of rhythm and single burst duration. Longevity of rhythms was defined as the time from start of recording until the time when the interval between consecutive bursts exceeded 1 min. Burst duration was defined, using Clampfit software (Molecular Devices, Union City, CA, USA), as the time interval from when the signal increased above and decreased below a threshold set at 10% of the peak amplitude value for that burst. Rhythms modified by changing superfusate cation composition or adding rolipram were analysed over a time period of 2 min at steady-state. Values are reported as means $\pm$ S.E.M. except for histological analyses where means $\pm$ S.D. were determined. Significance of values was determined by Student's one-sample *t* test using SigmaPlot (Systat software, Point Richmond, CA, USA). Significance was defined as $^*P < 0.05$ and $^{**}P < 0.01$.

Histology

For histological analysis after the experiments, both aspects of transected brainstem–spinal cords were fixed in phosphate buffer (1 : 2 mixture of 0.1 M NaH_2PO_4 + 0.1 M Na_2HPO_4 in H_2O, pH 7.2) containing 4% paraformaldehyde (all agents from Sigma). For staining after $>$ 15 min of fixation, preparations were incubated in phosphate buffer for at least 2 min and subsequently immersed 90 s for *en bloc* brainstems and slices and 45 s for 200–250 μm thick sagittal brainstem–pons slices in a solution consisting of 1% thionin acetate (Sigma)

in a mixture of 0.1 M sodium acetate trihydrate and 0.1 M acetic acid (Fisher). After staining, preparations were first 'washed' with phosphate buffer (2 min) and then with 50% ethanol (4 min) before returning to phosphate buffer for 2 min. Subsequently, preparations were transferred to a Petri dish and photographed (PL-A686 6.6 megapixel camera, Capture-SE software, PixeLINK, Ottawa, Ontario, Canada) in phosphate buffer under a stereo microscope (Zeiss-SR15, magnification ×32; Carl Zeiss, Jena, Germany).

Defined sectioning of brainstem–spinal cords

Brainstem–spinal cords with defined rostral boundary were generated using ventral brainstem surface landmarks (Fig. 1 and supplemental Fig. S1). Specifically, we found that the vagal nerve is located 0.06 ± 0.05 mm ($n = 5$) caudal to the caudal end of VII (VII_c) used as reference, whereas the location of the caudal cerebellar artery matches well with the rostral border of VII, i.e. 0.74 ± 0.16 mm ($n = 14$) *vs.* 0.76 ± 0.07 mm ($n = 16$) rostral to VII_c, respectively. The area covered by the most rostral hypoglossal nerve root spans the proposed (Smith *et al.* 1991; Ruangkittisakul *et al.* 2006) extension of the preBötC between 0.4 and 0.6 mm caudal to VII_c, with its rostral end located 0.41 ± 0.13 mm ($n = 5$) caudal to VII_c (Fig. 1 and supplemental Fig. S1).

preBötC slice boundaries can be determined 'online' by comparing respiratory marker nuclei in (pre)rhythmic slices with those in a reference brainstem atlas (Ruangkittisakul *et al.* 2006). The rostrocaudal locations of the marker structures, and thus slice boundaries, are referred to their distance from VII_c. Here, we used the atlas to identify the rostral boundary of transected brainstem–spinal cords (Fig. 1 and supplemental Figs S1–S3). This method was not suited to determine the boundary of preparations transected between VII_c and the inferior olive due to lack of marker structures. In these cases, the boundary was determined by measuring the distance in sagittal slices between VII_c and the caudal surface of the rostral aspects of the sectioned preparations (supplemental Figs S2 and S3). Analysis of the sagittal sections revealed a distance between inferior olive and VII_c of 0.16 ± 0.03 mm ($n = 5$), similar to our previous value (0.13 ± 0.03 mm, $n = 26$) based on 50 μm transverse serial sections (Ruangkittisakul *et al.* 2006).

Ventral respiratory column structures in newborn rat brainstem–spinal cords

As one major aim, we investigated the dependence of fictive respiratory rhythms in brainstem–spinal cords on their rostral boundary. We restricted our analysis to preparations without pons as influences of this structure on respiratory activity in this model were previously studied (Monteau *et al.* 1989; Errchidi *et al.* 1991; see also Alheid *et al.* 2004).

In the original voltage-sensitive dye imaging study on newborn rat brainstem–spinal cords, the pFRG was defined as a pre/postinspiratory active neuronal group, located ventrolateral to VII and close to the ventral surface (Onimaru & Homma, 2003). More recently, Onimaru *et al.* (2006) proposed that the pFRG may include regions up to ~0.2 mm caudal to VII_c (Fig. 1). Moreover, cells with pFRG-like activity pattern are also distributed caudal to that area (Arata *et al.* 1990; Smith *et al.* 1990; Ballanyi *et al.* 1999; Onimaru *et al.* 2003).

Compared to the RTN/pFRG, the preBötC was proposed to have a more defined rostrocaudal extension of ~0.2 mm, centred ~0.5 mm caudal to VII_c (Smith *et al.* 1991; Ruangkittisakul *et al.* 2006) (Fig. 1). Inspiratory neurons seem to be by far the major respiratory neuron class in thin preBötC slices. However, in less-reduced brainstem preparations a variety of respiratory neuron classes including pFRG-like cells are active within the region spanned by the preBötC (Arata *et al.* 1990; Smith *et al.* 1990; Schwarzacher *et al.* 1995; Sun *et al.* 1998; Onimaru *et al.* 2003; Paton *et al.* 2006). The area between preBötC and VII_c contains the BötC (Fig. 1) with a large number of expiratory neurons in addition to other types of respiratory cells (Feldman, 1986; Sun *et al.* 1998). Due to this overlap in the distribution of distinct respiratory neuron classes within the rostral ventrolateral respiratory column and other reasons, results from transection experiments should be interpreted with caution (Wilson *et al.* 2006).

Results

First, we studied inspiratory cervical nerve rhythms in three groups of brainstem–spinal cords with the boundary (i) slightly rostral to VII (thus including the BötC and RTN/pFRG), (ii) between VII and preBötC, and (iii) at or into the rostral preBötC border (Fig. 1).

Inspiratory cervical rhythm in transected brainstem–spinal cords

The mean boundary of six preparations with VII was 0.83 ± 0.08 mm rostral to VII_c (Fig. 2). In standard 1.2 mM Ca^{2+}, 3 mM K^+ solution, these brainstems generated cervical rhythm with an initial frequency of 6.9 ± 0.8 bursts min^{-1} and a burst duration of 0.60 ± 0.05 s (Fig. 2). After 3 h of recording, burst rate did not change (7.1 ± 0.35 bursts min^{-1}), whereas burst duration decreased to 0.40 ± 0.02 s. Raising superfusate K^+ from 3 to 6.2 mM (as in 'Suzue-type' solution) after the 5 h recording period reactivated rhythm, which stopped after 298 min in one preparation lacking ~10% of VII, and increased mean burst rate above control

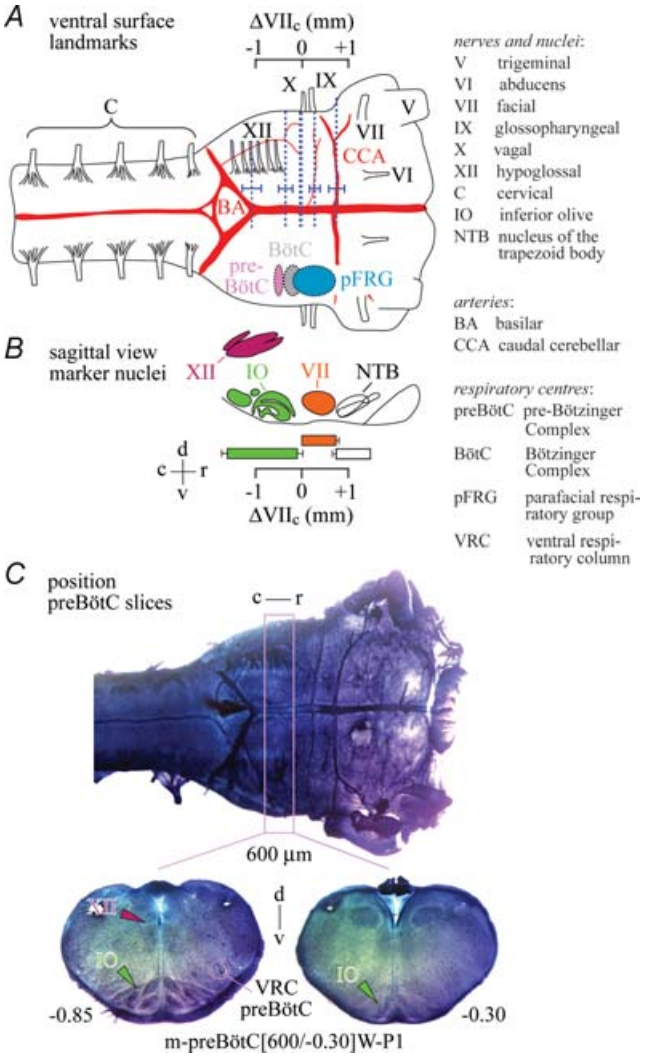

Figure 1. Regions of the ventral respiratory column and their ventral brainstem surface/nuclei landmarks in newborn rat brainstem–spinal cords

A, schematic drawing of ventral brainstem surface indicating the proposed locations of the pre-Bötzinger complex (preBötC), the Bötzinger complex (BötC) and the parafacial respiratory group (pFRG) of the ventral respiratory column (Alheid *et al.* 2004; Feldman & Del Negro, 2006). Vertical dotted lines and attached horizontal bars show means ± S.D. of the positions of surface structures in Sprague–Dawley (SD) and Wistar (W) rats of postnatal days (P) 0–4, specifically cranial nerves (IX, X, XII) and arteries (BA, CCA). The positions of BA, CCA, IX and XII were quantified (in mm) in reference to dotted line at X. The centre of the ∼0.2 mm spanning preBötC is presumably located 0.5 mm caudal to the caudal end of VII nucleus (VII$_c$) (+ and − signs indicating the location of structures rostral or caudal to VII$_c$, respectively), and the VII nucleus extends 0.76 mm rostrocaudally (Smith *et al.* 1991; Ruangkittisakul *et al.* 2006; supplemental Figs S1 and S2). The pFRG extends presumably from the rostral boundary of VII to ∼0.2 mm caudal to VII$_c$ (Onimaru & Homma, 2003, 2006; Onimaru *et al.* 2006). We found here that the caudal boundary of X nerve is located at VII$_c$, whereas the position of the CCA, at −0.74, matches well with the rostral end of VII. Furthermore, the proximal rostral boundary of the most rostral XII root coincides with the rostral preBötC border. The ΔVII$_c$ scale in *A* is positioned based on findings from cuts at levels including the BA, XII and X lines (supplemental Fig. S1). *B*, position projected onto a sagittal brainstem view of the respiratory marker nuclei IO, VII, XII (Ruangkittisakul *et al.* 2006) and NTB (supplemental Fig. S2). Scales in *A* and *B* have identical dimensions and positions, thus allowing comparison of respiratory structures relative to VII, XII, IO and NTB. *C*, most surface structures of *A* are seen in a fixed and thionin-stained SD–P2 brainstem. The pink box indicates the mean position of 600 µm thick 'm-preBötC slices' with the preBötC in the middle. The slice was labelled 'm-preBötC[600/−0.30]W–P1' (m, middle; 600, slice thickness in µm; −0.30, rostral boundary in mm; W–P1, rat strain and age). Here, we classified slices according to their rostral instead of caudal boundary in contrast to Ruangkittisakul *et al.* (2006) to allow for comparison with rostral boundaries of brainstem–spinal cord preparations. Other abbreviations: r, rostral; c, caudal; d, dorsal; v, ventral.

(8.7 ± 1.2 bursts min^{-1}, $n = 6$) with no stimulating effect on burst duration (Fig. 2).

The mean boundary of seven medullas cut between VII and preBötC was 0.25 ± 0.04 mm caudal to VII$_c$ (Fig. 3). The initial burst rate of 9.4 ± 0.7 bursts min^{-1} decreased to 8.1 ± 0.6 bursts min^{-1} within 20 min and remained rather stable for > 2 h in five cases. Burst duration decreased from initially 0.47 ± 0.02 s to 0.24 ± 0.06 s within 2 h, but remained stable thereafter (Fig. 3). In three preparations, rhythm stopped after 2–3 h, whereas four preparations showed rhythm for > 4 h (mean longevity 236 ± 26 min, $n = 7$). 6.2 mM K^+ and the cAMP-elevating agent rolipram (1 µM) reactivated rhythms with rates (6.7 ± 0.6 *vs.* 6.9 ± 0.9 bursts min^{-1}) and durations (0.45 ± 0.04 *vs.* 0.36 ± 0.08 s) very similar to control (Fig. 3).

The mean boundary of six preparations with rostrally exposed preBötC was 0.39 ± 0.04 mm caudal to VII$_c$ (Fig. 4). Initial burst rate was 9.3 ± 1.7 bursts min^{-1}, but decreased monotonically until rhythm stopped spontaneously (mean longevity 71.5 ± 14.1 min, $n = 6$). In three preparations still active after 80 min of recording, burst rate at that time was 3.3 ± 0.3 bursts min^{-1} and burst duration was 0.17 ± 0 s (Fig. 4). K^+ at 6.2 mM and rolipram (1 µM) reactivated rhythms with rates slightly lower than (7.5 ± 1.2 *vs.* 8.3 ± 0.5 bursts min^{-1}) and durations similar to (0.32 ± 0.07 *vs.* 0.30 ± 0.08 s) the initial value (Fig. 4).

Four preparations with the rostral boundary ≥ 0.45 mm caudal to VII$_c$, and thus likely to be very close to the preBötC centre (Fig. 1), did not generate respiratory rhythm in either 3 mM or 6.2 mM K^+. In three of these cases, elevated K^+ induced < 0.3 s irregular cervical nerve bursts with > 15 events min^{-1} and a distinct activity consisting of a > 1 min massive discharge (supplemental Fig. S4).

Analysis of pooled data from the above groups of brainstem–spinal cord preparations revealed a significant correlation between rostral boundary and longevity of rhythm, but not between boundary and burst rate, or initial frequency and longevity (Fig. 5).

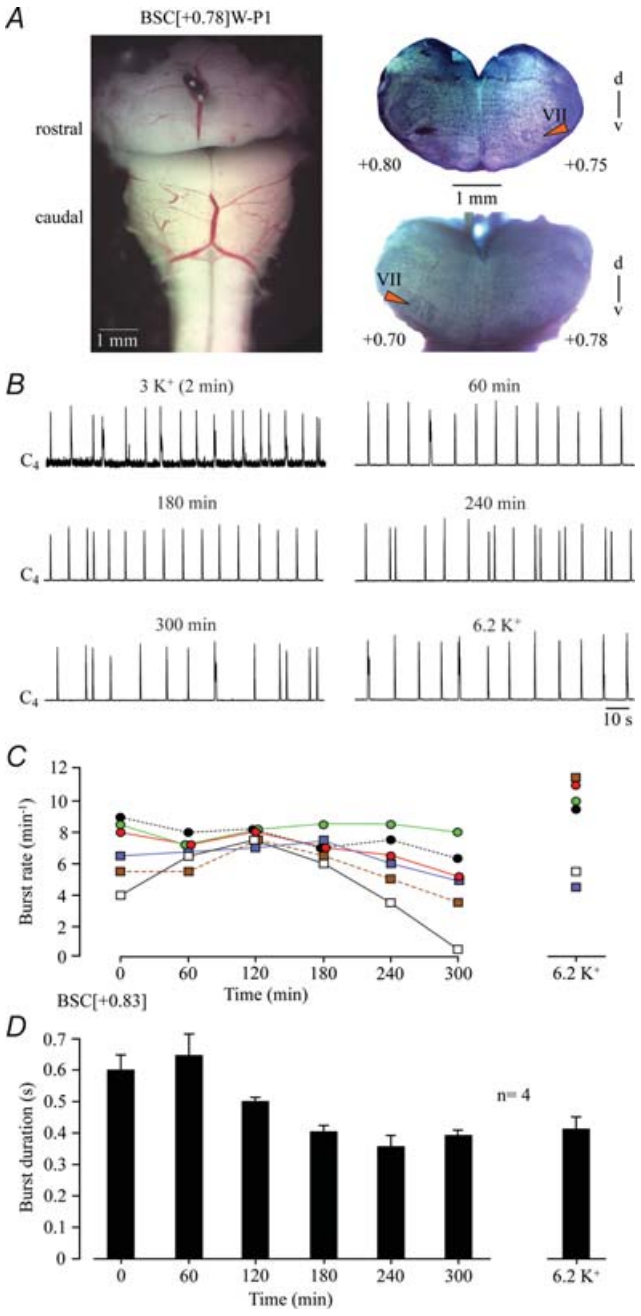

Figure 2. Cervical rhythm in 1.2 mM Ca^{2+}, 3 mM K^+ solution in brainstem–spinal cords with VII

A, left panel, transected brainstem–spinal cord (BSC) preparation from a P1 W rat with the rostral boundary 0.78 mm rostral to VII_c, thus a 'BSC[+0.78]W–P1', in standard saline after manual transection with a razor blade. Right panels, photographs of fixed and thionin-stained cut surfaces of corresponding rostral and caudal brainstem blocks after experiment. Numbers indicate transection level referred to VII_c (compare Fig. 1 and supplemental Fig. S1). The differing numbers on the left and right side of transection indicate a lateral tilt of the section plane. *B*, in the preparation of *A*, regular band-pass-filtered and integrated inspiratory-related bursting of the 4th ventral cervical (C_4) nerve rootlet was monitored for 5 h before superfusate K^+ level was raised to 6.2 mM. *C*, burst rates of 6 BSC with a mean boundary 0.83 rostral to VII_c (BSC[+0.83]). Note that rhythms slowed down slightly during the 4th hour of recording and stopped in one preparation shortly before 5 h (after 298 min). Raising K^+ to 6.2 mM after 5 h recording increased burst rates in all but one brainstems. *D*, burst duration in 4 preparations of *C*. Bars represent means and S.E.M. Numbers in the left part of the abscissa indicate the time period after start of recording.

Pre/postinspiratory lumbar rhythm in transected brainstem–spinal cords

In a further approach, we studied the dependence of pre/postinspiratory lumbar nerve bursting (Janczewski *et al.* 2002) on the rostral boundary of *en bloc* brainstems with complete spinal cord. Ten preparations with boundaries < 0.6 mm rostral to VII_c, thus containing $< 79\%$ of VII, did not show pre/postinspiratory lumbar bursting, but generated regular cervical inspiratory rhythm (Fig. 6). On the contrary, seven preparations with boundaries > 0.6 mm rostral to VII_c showed both pre/postinspiratory lumbar and inspiratory cervical nerve bursting (Fig. 6).

Hypoglossal nerve activity in transected brainstem–spinal cords

Next, we assessed whether inspiratory hypoglossal rhythms in *en bloc* preparations also depend on the transection level. In five preparations cut between preBötC and VII_c (mean boundary 0.20 ± 0.04 mm caudal to VII_c), burst rates in 3 mM K^+ of synchronous rhythms in cervical and most rostral hypoglossal nerve roots were identical. After an initial time period of 8.7 ± 1.1 bursts min^{-1}, burst rate stabilized at 7.1 and 7.7 bursts min^{-1} between 20 and 120 min, but decreased to 4.8 ± 1.0 and 4.8 ± 1.3 bursts min^{-1} at 180 and 240 min, respectively (Fig. 7). The amplitude of rostral hypoglossal root bursts was stable during recording periods > 4 h in some cases (Figs 7 and 8). Also their duration remained stable at $\sim$0.4 s, whereas cervical burst duration decreased from $\sim$0.4 s to < 0.3 s after 1 h of recording (Fig. 7). Hypoglossal burst duration was also similar to control when rhythm was reactivated after spontaneous arrest by elevated K^+ (6.2, 7, 9 mM) or rolipram (1 μM), all of which restored cervical burst duration to control values (Fig. 7). Only 9 mM K^+ increased the burst rate of re-evoked rhythms above initial control values. Under all these conditions, hypoglossal and cervical rhythms showed 1 : 1-coupling (Fig. 7). Neither K^+ nor rolipram affected the amplitude of hypoglossal or cervical bursting. In 12 additional preparations with similar boundaries caudal to VII_c, the amplitude of bursting of rostral hypoglossal roots remained constant or increased during the first hour of recording (Fig. 8).

In contrast, burst amplitude, but not duration, decreased within 20–90 min after start of recording

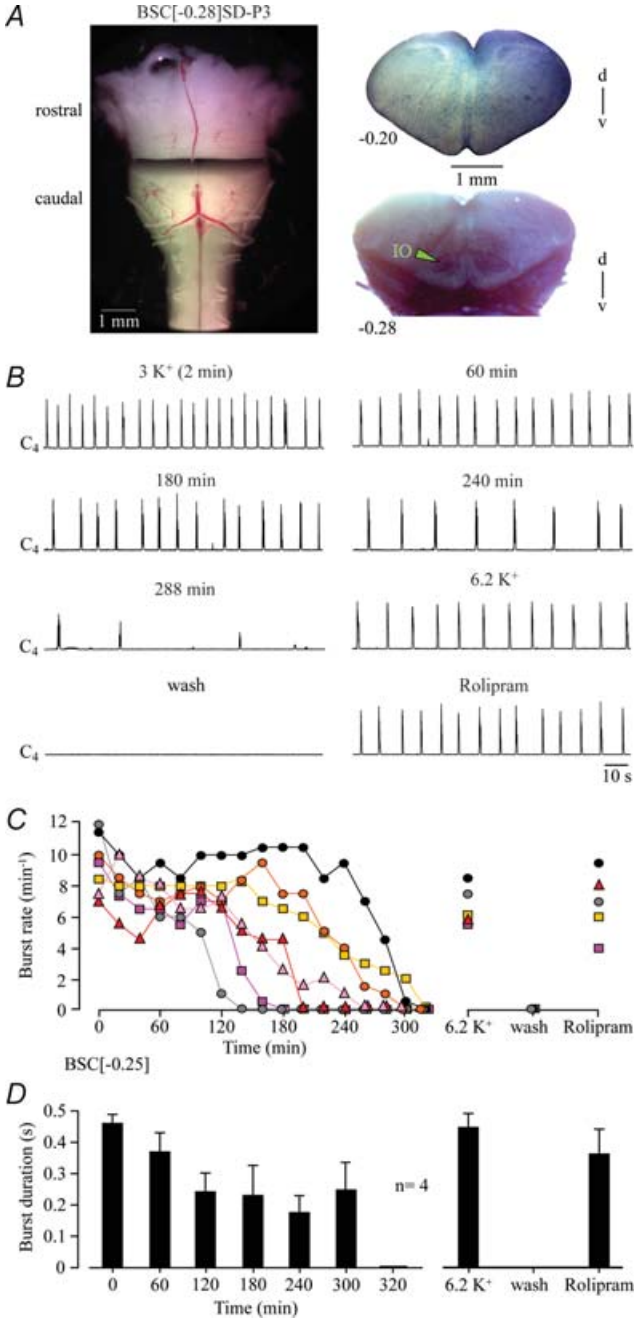

Figure 3. Cervical rhythm in brainstem–spinal cords cut between preBötC and VII
A, left panel, transected BSC[−0.28]SD–P3 preparation. Right panels, fixed and thionin-stained cut surfaces of corresponding rostral and caudal brainstem blocks. *B*, between 3 and 4 h of recording, inspiratory C_4 nerve bursting slowed down notably before rhythm stopped spontaneously after 288 min (last bursts shown). Very similar rhythm was reactivated by raising superfusate K^+ to 6.2 mM and, after return to 3 mM K^+ saline, by bath-application of the cAMP-elevating agent rolipram (1 μM). *C*, burst rates of 7 BSC[−0.25]. Note that rhythm persisted in 5 preparations for > 3 h. *D*, burst duration in 4 preparations of *C* with very similar mean rostral boundary (BSC[−0.26]). Bars represent means and S.E.M. Numbers in the left part of the abscissa indicate the time period after start of recording.

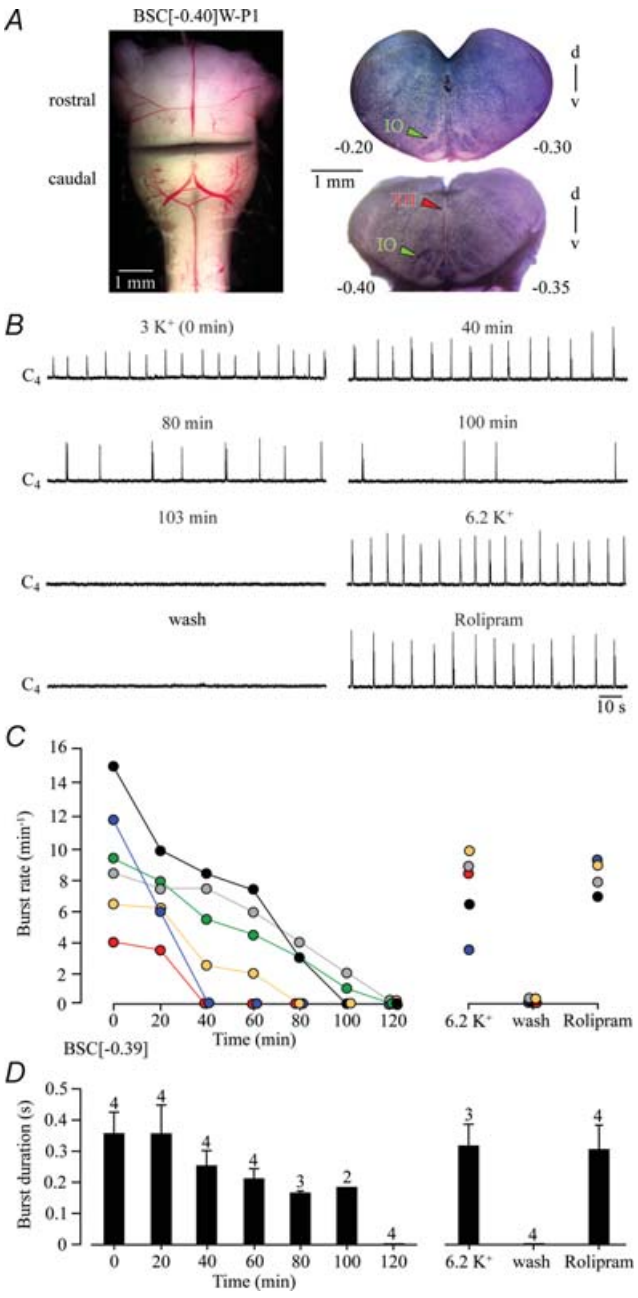

Figure 4. Cervical rhythm of brainstem–spinal cords with boundaries at or into the rostral preBötC border
A, left panel, transected BSC[−0.40]W–P1 preparation. Right panels, fixed and thionin-stained cut surfaces of corresponding brainstem blocks. *B*, C_4 bursting was revealed for > 1 h before rhythm stopped after 103 min. Very similar rhythm was reactivated by 6.2 mM K^+ and, after return to 3 mM K^+, bath-application of rolipram (1 μM). *C*, burst rates of 6 BSC[−0.39]. Note that rhythm stopped spontaneously after time periods of 40–120 min. *D*, burst duration in 4 preparations of *C*. Bars represent means and S.E.M. Digits above bars indicate number of (still active) preparations tested. Numbers in the left part of the abscissa indicate the time period after start of recording.

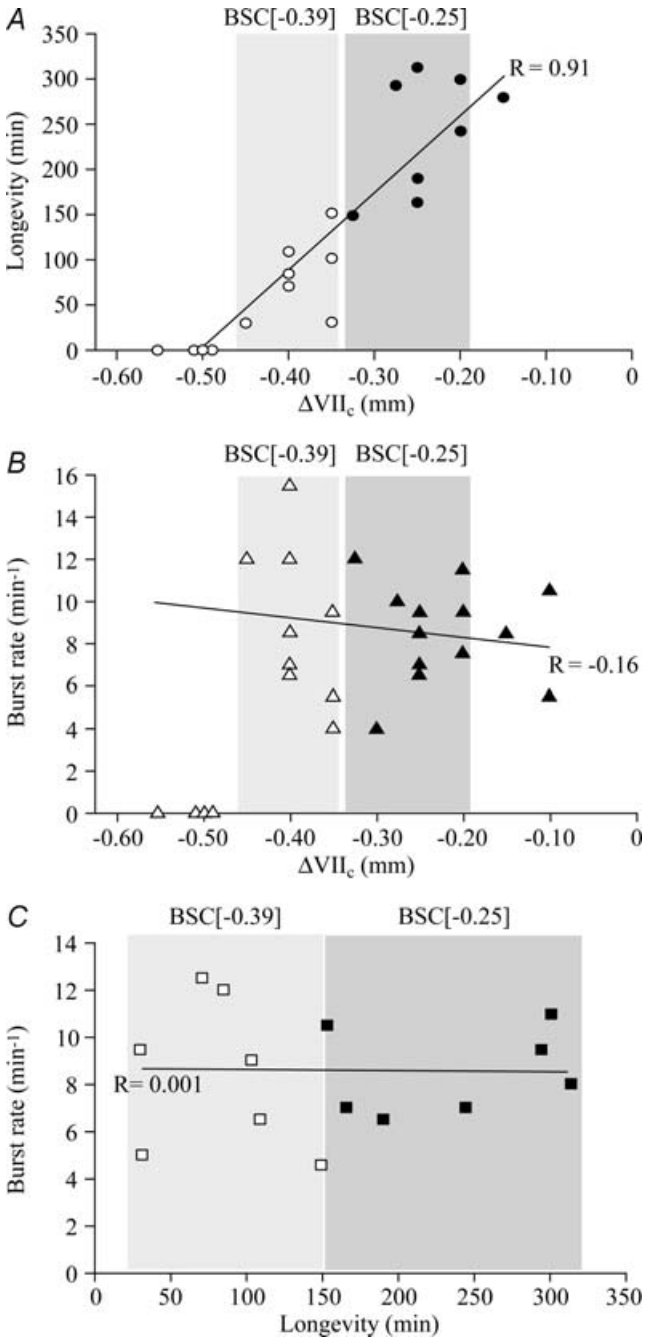

Figure 5. Correlation between rostral boundary, longevity and burst rate of cervical rhythm in brainstem–spinal cords
A, significant ($P < 0.01$) correlation between the longevity of cervical inspiratory rhythm and rostral boundary (*R* is correlation coefficient). In contrast, no significant correlations were revealed between burst rates (determined after 10 min of recording) and rostral boundaries (*B*) or longevity of rhythm (*C*). Grey areas indicate the two groups of preparations used for the analyses in Figs 3 and 4. Note that preparations with the rostral boundary at −0.50 or more caudal (thus caudal to the proposed preBötC centre) did not show respiratory rhythm (compare supplemental Fig. S4). *A* and *C* contain less data points compared to *B* as longevity was not tested in all preparations.

in caudal hypoglossal roots of brainstem–spinal cords without VII (Fig. 8). Bursting disappeared in 1 of 4 preparations and stabilized after ∼1 h in the other cases at 17 ± 6.9% of the initial value. In four preparations with VII (mean boundary 0.11 ± 0.07 mm rostral to VII$_c$), amplitude of rostral hypoglossal root bursts fell to 23 ± 4.7% of initial values after 20–50 min of recording. Furthermore, the depression was more pronounced (6.8 ± 2.8%) after similar time periods in four preparations with complete VII (Fig. 8).

Rhythm in preBötC slices

Next, we compared inspiratory-related rhythms in 1.2 mM Ca^{2+} and 3 mM K^+ between *en bloc* medullas and 600 μm m-preBötC slices with a mean rostral boundary 0.24 ± 0.11 mm ($n = 5$) caudal to VII$_c$. The initial rate of bursting in the region of the ventral respiratory column containing the preBötC was 7.2 ± 1.0 bursts min^{-1}, but decreased within 20 min to 5.2 ± 0.8 bursts min^{-1}. Burst rate remained approximately at that value until rhythm stopped after 60–140 min (mean longevity 87.8 ± 16.8 min, $n = 5$) (Fig. 9). preBötC burst duration fluctuated between 0.5 and 0.8 s within the first 80 min of recording. As with cervical bursts in *en bloc* medullas, the rate of hypoglossal bursts was 1 : 1-coupled to preBötC activity, while their duration was shorter and decreased from an initial value of 0.39 ± 0.07 to 0.30 ± 0.14 after

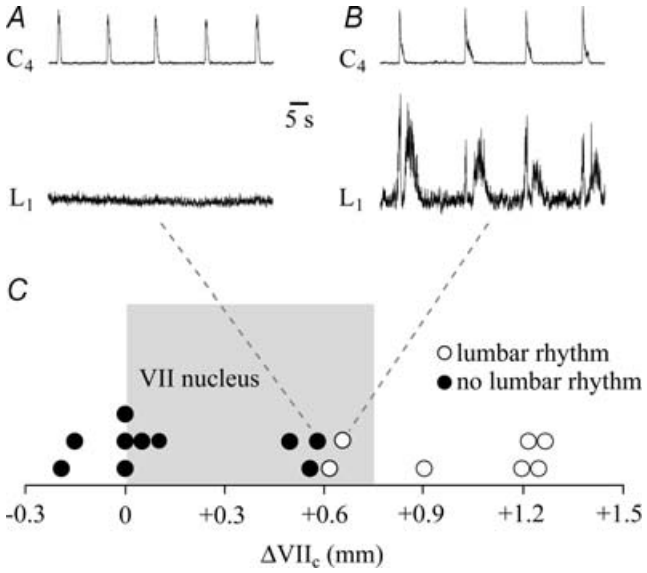

Figure 6. Dependence of pre/postinspiratory lumbar nerve bursting on rostral boundary of brainstem–spinal cords
A, a BSC[+0.58]W–P1 preparation generated stable inspiratory C_4 bursting, but did not show respiratory-related activity in the first ventral lumbar (L_1) root. *B*, pre/postinspiratory L_1 bursting was revealed in a BSC[+0.67]W–P0. *C*, plot of the occurrence (○) or absence (●) of lumbar pre/postinspiratory rhythm *vs.* the rostral boundary. Grey area indicates the rostrocaudal extension of VII (compare Fig. 1).

1 h (Fig. 9). After spontaneous arrest, preBötC and hypoglossal rhythms were restored by 6.2 mM K^+ or rolipram (1 μM) with rates comparable to those in 3 mM K^+ 20–40 min after start of recording. While the duration of K^+-induced preBötC and hypoglossal bursts was also similar to control, rolipram-induced bursts were shorter (Fig. 9).

The limited longevity of slice rhythms in standard 1.2 mM Ca^{2+} and 3 mM K^+ solution contrasted with ~4 h longevity of rhythm in m-preBötC slices with similar boundaries in our previous study (Ruangkittisakul *et al.* 2006). Thus, we tested next whether this difference may be due to use of 1 mM instead of 1.2 mM Ca^{2+} in that report. Indeed, rhythm in five slices with the rostral boundary 0.21 ± 0.08 mm caudal to VII_c lasted > 2 h and even > 3 h in three of these cases in 1 mM Ca^{2+}. Thus, longevity was significantly greater (211.4 ± 39.2 min, $P < 0.05$) in 1 mM

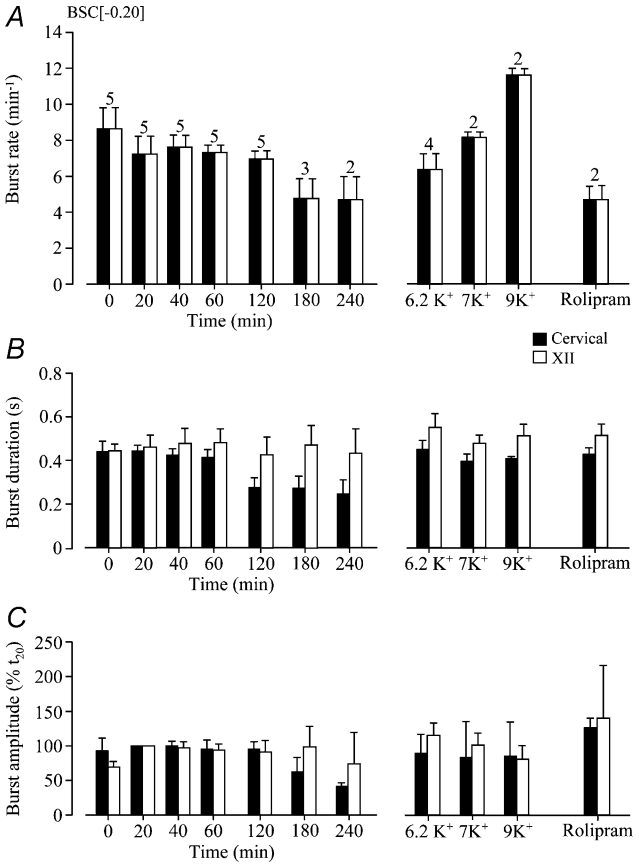

Figure 7. Statistical analysis of cervical and hypoglossal rhythms in brainstem–spinal cords without VII
A, in 5 BSC[−0.20] preparations, rhythms in cervical roots (open bars) and most rostral hypoglossal (XII) roots (filled bars) had identical burst rates indicating a 1 : 1 coupling ratio. As evident from numbers above bars, rhythm stopped in 2 and 3 preparations before 3 and 4 h of recording, respectively. Identical burst rates were also revealed upon reactivation of rhythm with elevated K^+ or rolipram (1 μM). *B*, XII burst duration was similar during both long-term recording and re-stimulation of rhythm. In contrast, cervical burst duration decreased during the first hour of recording, but was restored by raised K^+ and rolipram. *C*, cervical burst amplitude decreased after 2 h of recording, but was re-increased by the stimulatory procedures. XII burst amplitude referred to the value at 20 min (t_{20}) was stable under all conditions. Numbers of preparations above bars in *A* are identical to those in *B* and *C*.

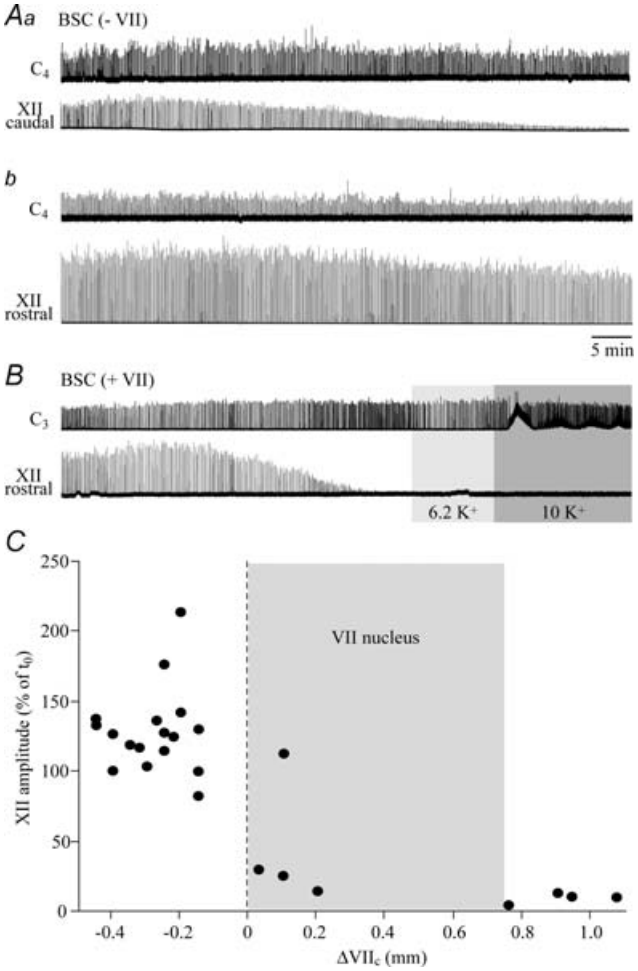

Figure 8. Dependence of XII rhythm on rostral boundary of brainstem–spinal cords
A, in a BSC[−0.15]SD–P2 preparation, cervical rhythm monitored within < 2 min after transfer to the experimental chamber (*Aa*) was stable for > 1 h. In contrast, the amplitude of synchronous bursting in a caudal XII root started to decrease after ~17 min and reached < 10% of the initial amplitude after 1 h. *Ab*, changing the suction electrode from the caudal to the most rostral XII root within < 5 min after end of the recording in *Aa* revealed robust bursting. The amplitude of most rostral XII root bursts remained at > 70% of the initial value for the illustrated time period and continued for > 2 h at similar levels afterwards. *B*, in a BSC[+1.1]SD–P1 preparation, cervical rhythm monitored within < 2 min after transfer to the experimental chamber was stable for > 1 h, whereas bursting of the most rostral XII root started to decrease in amplitude ~17 min after start of the recording and disappeared after ~35 min. XII rhythm could not be reactivated by raising superfusate K^+ from 3 mM to 6.2 or 10 mM. Same time scale in *A* and *B*. *C*, plot of XII nerve burst amplitude after 1 h, referred to the value at the start of recording (t_0) *vs.* rostral boundary. Grey area indicates the rostrocaudal extension of VII nucleus (compare Figs 1 and 6).

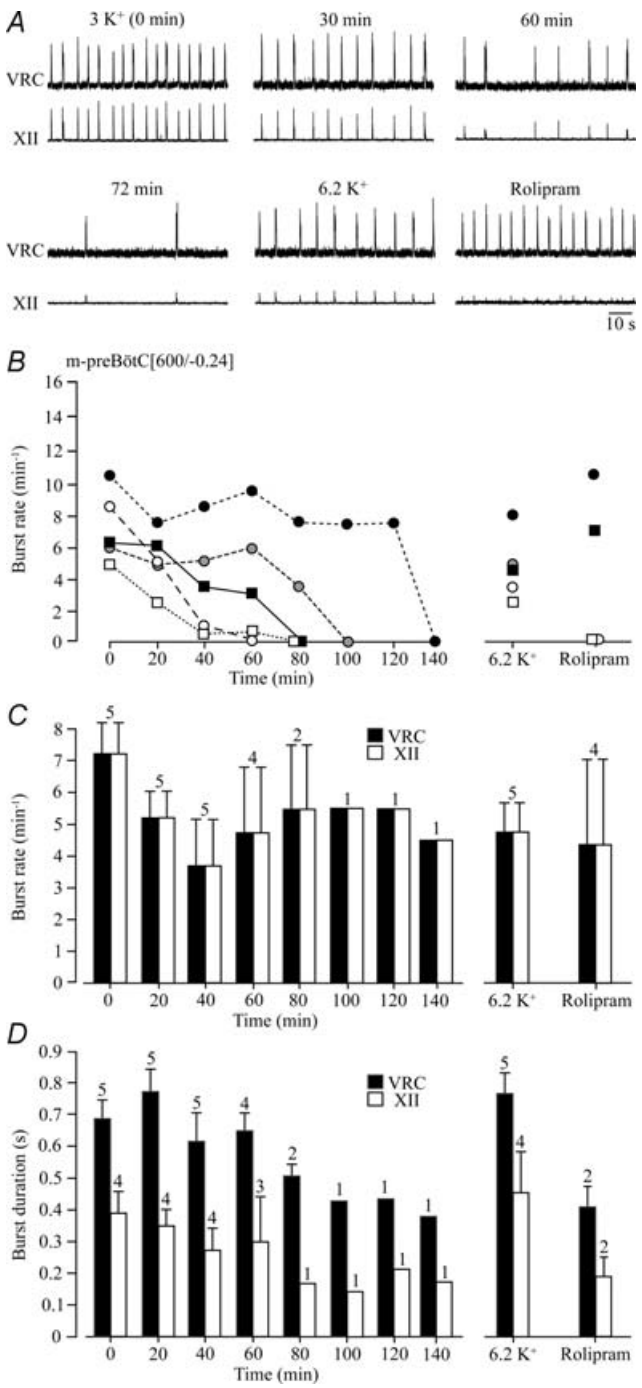

Figure 9. preBötC and XII rhythms in preBötC slices in 1.2 mM Ca^{2+} and 3 mM K^+

A, bursting within the ventral respiratory column (VRC), neighbouring the preBötC and reflecting its activity, showed 1 : 1-coupling to XII nerve bursting in a m-preBötC[600/−0.10]W–P2 slice in standard solution. Following spontaneous arrest of rhythm after 72 min (last bursts shown), 1 : 1-coupled bursting was reactivated by raised K^+ and, after return to 3 mM K^+ solution, rolipram (1 μM). *B*, burst rates in 5 m-preBötC[600/−0.24] slices with mean rostral/caudal boundaries $0.24 \pm 0.11/0.86 \pm 0.05$ mm caudal to VII_c show that rhythm lasted for > 80 min in only 2 slices. Rhythm was effectively reactivated in all slices by 6.2 mM K^+, whereas rolipram (1 μM) was only effective in 2 of 4 slices tested. *C*, mean values of burst rates in *B* show 1 : 1-coupling between XII and VRC/preBötC bursts under all conditions. *D*, mean burst durations reveal that VRC/preBötC bursts are notably longer than XII bursts.

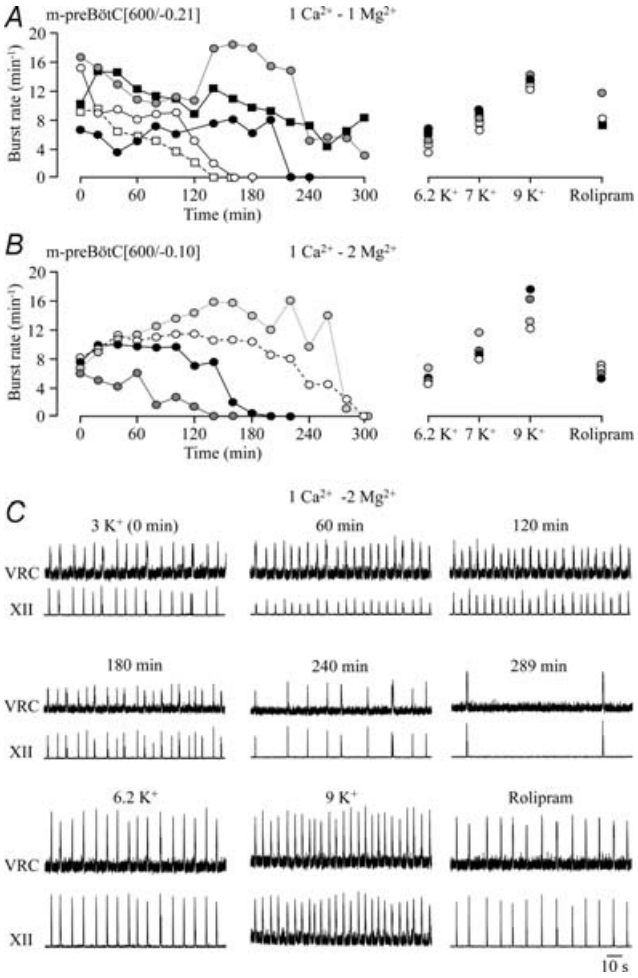

Figure 10. preBötC and XII bursting in preBötC slices in 1 mM Ca^{2+} and 3 mM K^+

A, rhythm in 5 m-preBötC[600/−0.21] slices with mean rostral/caudal boundaries $0.21 \pm 0.08/0.82 \pm 0.04$ mm caudal to VII_c kept in superfusate with 3 mM K^+, 1 mM Ca^{2+} and 1 mM Mg^{2+} persisted for extended time periods, in 2 cases > 4 h. *B*, rhythm with similar burst rate and longevity was seen in 4 m-preBötC[600/−0.10] slices with mean rostral/caudal boundaries $0.10 \pm 0.07/0.71 \pm 0.06$ mm caudal to VII_c in superfusate with 3 mM K^+, 1 mM Ca^{2+} and 2 mM Mg^{2+}. Rhythm was effectively reactivated after spontaneous arrest by 6.2, 7 and 9 mM K^+ and rolipram (1 μM). *C*, the recording from a m-preBötC[600/−0.05]W–P2 slice included in *B* shows a 1 : 1-coupling of VRC/preBötC and XII rhythms during spontaneous and re-evoked activity. Note that the recording in rolipram was done 8 h after start of recording and that the amplitude of XII bursting fluctuated during the first 120 min after start of recording.

Ca^{2+} compared to slices in 1.2 mM Ca^{2+} (Fig. 10). Also in 1 mM Ca^{2+}, hypoglossal bursts showed 1 : 1-coupling to preBötC bursting, but their amplitude fluctuated by ∼40% with a period of 20–40 min in two slices. Rhythm

was effectively restored after spontaneous arrest by both K^+ (6–9 mM) and rolipram (1 μM) (Fig. 10).

Next, we studied whether slice rhythms are modified by raising Mg^{2+} from 1 to 2 mM as was used by Ruangkittisakul *et al.* (2006). In four slices with mean rostral boundary 0.10 ± 0.07 mm caudal to VII_c, longevity of rhythm (216 ± 37.1 min, $n = 4$) was very similar in 1 mM Ca^{2+}, 2 mM Mg^{2+} to that in 1 mM Ca^{2+}, 1 mM Mg^{2+} slices and significantly ($P < 0.05$) greater than in 1.2 mM Ca^{2+}, 1 mM Mg^{2+} slices. Also two of these slices showed fluctuations in hypoglossal burst amplitude (Fig. 10). In three slices, synchronous preBötC and hypoglossal rhythms were stable for > 3 h, in two cases for > 4 h (Figs 10 and 11). Burst rates during these time periods ranged from 7 to 9.4 bursts min^{-1}, which was higher than in 1.2 mM Ca^{2+} (after 40–60 min). The duration of preBötC and hypoglossal bursts decreased from initially 0.75 ± 0.06 s to 0.49 ± 0.03 s and 0.45 ± 0.06 s to 0.21 ± 0.08 s after 3 h, respectively (Fig. 11). After spontaneous arrest, rhythm of similar burst duration was restored by K^+ (6.2, 7, 9 mM) or rolipram (1 μM). K^+ at 6.2 mM and 7 mM as well as rolipram restored bursting at rates similar to control, whereas 9 mM K^+ induced a faster rhythm at $\sim$15 bursts min^{-1} (Fig. 11).

Ca^{2+} sensitivity of inspiratory rhythms in transected brainstem–spinal cords

As one major finding, inspiratory-related rhythms in *en bloc* medullas with distinct rostral boundaries shared various features with those in preBötC slices. These features included a similar limited longevity of rhythms in brainstem–spinal cords with exposed preBötC and m-preBötC slices. In the slices, longevity and burst rate were greatly enhanced by lowering superfusate Ca^{2+} from 1.2 mM to 1 mM. This suggests that, conversely, raising Ca^{2+} above 1.2 mM may depress preBötC-related (motor) rhythms. In the Introduction, we hypothesized that raised Ca^{2+} may be responsible for block of cervical rhythms in transected brainstem–spinal cords. The studies reporting such block (Onimaru & Homma, 1987; Onimaru *et al.* 2006) used 'Suzue-type' solution containing 2.4 mM Ca^{2+} and also higher K^+ (6.2 mM) and Mg^{2+} (1.3 mM) compared to the standard solution used here.

We tested the effects of this solution on five brainstem–spinal cord preparations that were transected between preBötC and VII. Raising first K^+ from 3 to 6.2 mM changed neither the rate nor the duration of cervical bursts, whereas subsequent elevation of Ca^{2+} (from 1.2 to 2.4 mM) and Mg^{2+} (from 1 to 1.3 mM) blocked rhythm within < 10 min (Fig. 12). Rhythm with a rate and burst duration similar to control was reactivated in that solution by 10 mM K^+, whereas 8 mM K^+ was less effective (Fig. 12). Six preparations cut more caudally (at the rostral preBötC border) responded similarly. However, 10 mM K^+ reactivated rhythm with a burst duration similar to controls, but at a lower rate, and 8 mM K^+ did not restore bursting (Fig. 12). This high Ca^{2+}/K^+ (Mg^{2+}) solution also modified non-respiratory activity in three preparations with boundaries ≥ 0.45 mm caudal to VII_c that did not generate respiratory rhythm (supplemental Fig. S4).

The fact that Ca^{2+} was doubled, whereas Mg^{2+} was raised by only 30%, suggests that Ca^{2+} is responsible for depression of cervical rhythm. To test this, eight preparations with exposed preBötC were kept in 6.2 mM K^+ to maintain stable rhythm and were superfused with

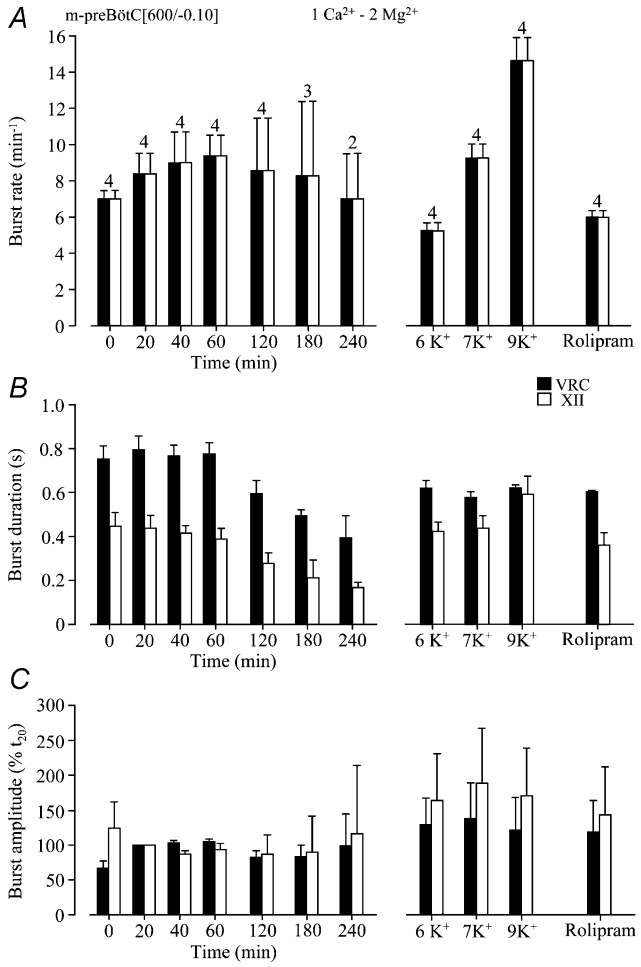

Figure 11. Statistical analysis of preBötC and XII rhythms in preBötC slices in 1 mM Ca^{2+} and 3 mM K^+
A, the 4 m-preBötC[600/−0.10] slices of Fig. 10*B* showed a 1 : 1-coupling of VRC/preBötC and XII nerve bursting. Note that burst rate slightly increased during the first hour of recording and that 9 mM K^+ restored rhythm of $\sim$50% higher burst rate than the initial rhythm in 3 mM K^+. *B*, the durations of both VRC/preBötC and XII bursts decreased following the first hour of recording. Both, K^+ and rolipram (1 μM) re-stimulated burst durations. *C*, the amplitude of VRC/preBötC and XII bursts, referred to the value at 20 min (t_{20}), was stable in control solution, whereas elevated K^+ and rolipram had an augmenting effect. Numbers of slices shown above bars in *A* are identical to those in *B* and *C*.

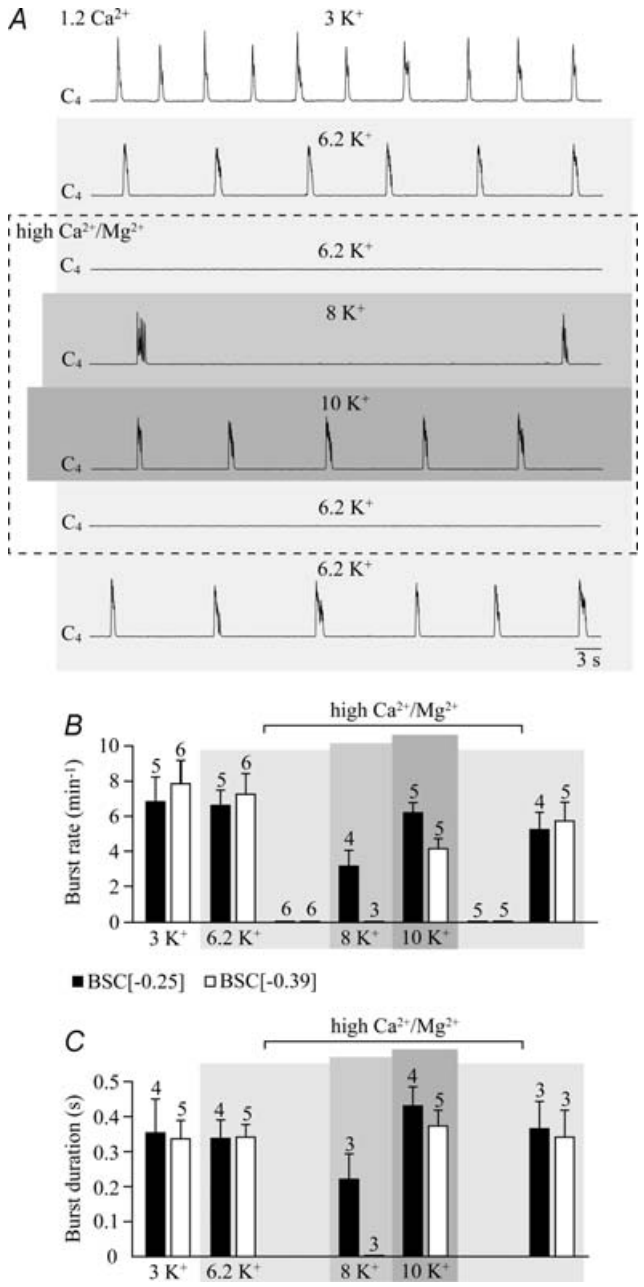

Figure 12. Block by high Ca^{2+}/K^+ (Mg^{2+}) solution of cervical rhythm in brainstem–spinal cords without VII
A, in a BSC[−0.28]SD–P3, elevating superfusate Ca^{2+} from 1.2 to 2.4 mM and Mg^{2+} from 1.0 to 1.3 mM (3rd trace from top) abolished the inspiratory rhythm which was previously stable in both 3 mM (top trace) and 6.2 mM K^+ (2nd trace from top). Rhythm very similar to control was reactivated in 2.4 mM Ca^{2+} and 1.3 mM Mg^{2+} by raising K^+ further, to 10 mM (5th trace from top), whereas 8 mM K^+ was less effective (4th trace from top). Rhythm was blocked again after return to 6.2 mM K^+, 2.4 mM Ca^{2+} and 1.3 mM Mg^{2+} solution (2nd trace from bottom) and recovered effectively in 6.2 mM K^+, 1.2 mM Ca^{2+} and 1 mM Mg^{2+} (bottom trace). *B* and *C*, mean rates (*B*) and durations (*C*) of cervical bursts in two sets of preparations with different mean rostral boundaries, specifically BSC[−0.25] and BSC[−0.39]. Digits above bars indicate the number of preparations tested. Only a subset of preparations in *B* was used for the analysis in *C*. Bars represent means and S.E.M.

1.8 mM Ca^{2+} at constant Mg^{2+} (1 mM). This modest Ca^{2+} rise by 0.6 mM decreased burst rate within < 10 min from 5.5 ± 0.9 to 1.1 ± 0.4 bursts min^{-1} ($P < 0.01$; block of rhythm in 3 cases) (Fig. 13). The inhibition by Ca^{2+} of cervical rhythm was accompanied in > 50% of cases by non-respiratory bursting that was absent, or less pronounced, in hypoglossal recordings (Fig. 13). Thus, Ca^{2+} effects were quantified by analysing only synchronous cervical and hypoglossal bursts, which were 1 : 1-coupled during both control and raised Ca^{2+} (Fig. 13).

In four of the preparations exposed to 1.8 mM Ca^{2+}, a subsequent Ca^{2+} rise to 2 mM depressed rhythm further to 0.3 ± 0.3 bursts min^{-1} ($P < 0.01$; block of rhythm in 3 cases) (Fig. 14). Rhythm reappeared at 4.8 ± 0.5 bursts min^{-1} with burst duration similar to control in 10 mM K^+ after block by 2 mM Ca^{2+}, whereas 8 mM K^+ was less effective (2.4 ± 1.1 bursts min^{-1}).

In contrast to preparations transected between VII and preBötC, cervical rhythm in 6.2 mM K^+ was not blocked by 1.8–2.4 mM Ca^{2+} in preparations with (portions of) VII (Figs 13 and 14). The $[Ca^{2+}]$ to effectively depress or abolish rhythm increased significantly with increasing amount of tissue rostral to the preBötC (Fig. 14).

Ca^{2+} block of preBötC slice rhythm

The latter results in brainstem–spinal cord preparations suggested that the capability of the preBötC to generate rhythm in moderately elevated K^+ is substantially impaired by raising Ca^{2+} by only 0.6 mM. In a final approach, we investigated whether preBötC bursting and inspiratory motor rhythm in slices with robust longevity in 1 mM Ca^{2+} and 3 mM K^+ have a similarly high sensitivity to acutely elevated superfusate Ca^{2+}.

In 10 slices with a mean rostral boundary 0.19 ± 0.10 caudal to VII_c, raising Ca^{2+} from 1 to 1.5 mM depressed within 10–15 min the rate of 1 : 1-coupled preBötC and hypoglossal bursting from 8.1 ± 0.8 to 1.2 ± 0.4 bursts min^{-1} ($P < 0.01$; block of rhythm in 4 cases) (Fig. 15). Both rhythms started to recover within 10–20 min after return to 1 mM Ca^{2+}, but mean recovery was < 50% of control even after 30 min of washout of 1.5 mM Ca^{2+}. The incomplete recovery of burst rates was not caused by time-dependent spontaneous slowing of rhythm in 3 mM K^+ as inspiratory frequency was stable during comparable time periods in seven control slices with a mean rostral boundary 0.18 ± 0.11 mm caudal to VII_c (Fig. 15).

For comparison with our findings in brainstem–spinal cords, the effects of 1.8 mM Ca^{2+} in 6.2 mM K^+ were tested in six m-preBötC slices with a mean rostral boundary 0.26 ± 0.12 mm caudal to VII_c. Synchronous preBötC and hypoglossal burst rates were depressed by 1.8 mM Ca^{2+} from 6.1 ± 0.8 to 0.2 ± 0.2 bursts min^{-1} ($P < 0.01$;

block of rhythm in 5 cases). Elevating K^+ to 8 mM and 10 mM reactivated both types of rhythms at 3.2 ± 0.7 and 10.1 ± 1.9 bursts min^{-1}, respectively, with burst durations similar to control (Fig. 15).

Discussion

Inspiratory-related rhythms in newborn rat brainstem–spinal cords containing the preBötC inspiratory centre (plus more rostral respiratory regions) and preBötC slices were similar in physiological Ca^{2+}/K^+ solution. The reduced longevity of inspiratory rhythms in *en bloc* preparations with exposed preBötC and slices is caused by a strong extracellular Ca^{2+}/K^+ antagonism. We discuss whether the absence of pre/postinspiratory rhythms in brainstems lacking a major portion of VII may be due to reduction of the RTN/pFRG, whereas block of hypoglossal bursting in preparations with (portions of) VII may possibly result from interstitial accumulation of inhibitory neuromodulator(s).

Implications from defined sectioning of isolated brainstem–spinal cords

In early postnatal rats, the constancy of rostrocaudal extensions of marker brainstem nuclei enables the generation of preBötC slices with defined boundaries (Ruangkittisakul *et al.* 2006). Based on a similar constancy of ventral brainstem surface landmarks, we generated here brainstem–spinal cords with a defined rostral boundary. Such preparations with rostrally exposed preBötC allow the study of how the preBötC drives hypoglossal and spinal motor networks with as little as possible interference from the more rostral BötC and RTN/pFRG. Also preBötC interactions with the RTN/pFRG and/or BötC should be studied in defined preparations where the extension of the rostral ventral respiratory column can be determined within a few tens of micrometres. The finding of stable cervical rhythm in *en bloc* preparations cut between VII and preBötC is very similar to our previous report (Smith *et al.* 1991). As discussed below, use of 2–2.4 mM Ca^{2+} (instead of 1.5 mM Ca^{2+} in the latter study) explains depression/block of rhythm observed by others upon similar transection (Onimaru & Homma, 1987; McLean & Remmers, 1994; Onimaru *et al.* 2006).

Despite caveats (Wilson *et al.* 2006), sectioning experiments can increase understanding of structure–function relationships of respiratory networks. For example, the RTN/pFRG in the rostral aspect of transected newborn rat medullas remained functional without the preBötC (Onimaru *et al.* 2006). Furthermore, transection close to VII_c abolished expiration in juvenile

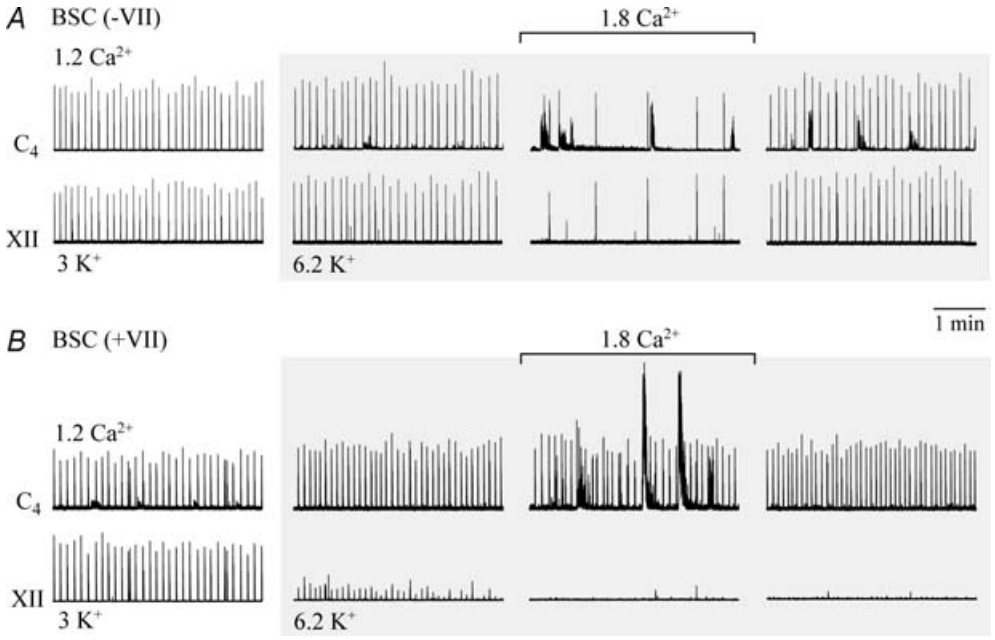

Figure 13. Different sensitivity to raised superfusate Ca^{2+} of inspiratory rhythms in brainstem–spinal cords without or with VII
A, in a BSC[−0.25]SD–P3 without VII, raising Ca^{2+} from 1.2 to 1.8 mM after changing from 3 to 6.2 mM K^+ reversibly depressed both cervical and XII inspiratory rhythms. Note the occurrence of pronounced non-respiratory activity in the cervical, but not the XII recording during 1.8 mM Ca^{2+}. *B*, 1.8 mM Ca^{2+} did not depress cervical rhythm in a BSC[+0.75]W–P1 preparation with complete VII, but induced large amplitude non-respiratory activity. Note that XII rhythm was stable in *A*, whereas it disappeared in *B* during the time period of raising K^+. Same time scale in *A* and *B*.

rats *in vivo* (Janczewski & Feldman, 2006). Those authors hypothesized that breathing is generated by anatomically separate rhythm generators, one generating active expiration located close to VII in the region of the RTN/pFRG, the other generating inspiration located more caudally in the preBötC. The latter study supported the conclusion from a previous combined *in vivo*/*in vitro* report that the pFRG ultimately drives expiratory abdominal muscles *in vivo* via ipsilateral medullary premotoneurons located caudal to the preBötC that project to contralateral pre/postinspiratory lumbar motoneurons (Janczewski *et al.* 2002). The findings of Janczewski & Feldman (2006) also support the hypothesis, based on a differential sensitivity *in vivo* and *in vitro* of preBötC- and pFRG-related rhythms to opioids, that these rhythmogenic respiratory groups form a functionally coupled dual respiratory centre (Mellen *et al.* 2003). We found that the brainstem level critical for pre/postinspiratory lumbar bursting is close to the rostral and not caudal end of VII, at least in isolated neonatal rat brainstems. It cannot be concluded though that pFRG networks, which presumably generate this expiratory motor behaviour, are only located rostral to that sectioning level. For example, if the axons of caudal RTN/pFRG interneurons or premotoneurons project rostrally first, cutting would affect this pathway.

Modulation of preBötC rhythms by neighbouring brainstem regions

Burst rates of cervical rhythm in physiological Ca^{2+}/K^{+} did not substantially differ between *en bloc* medullas with

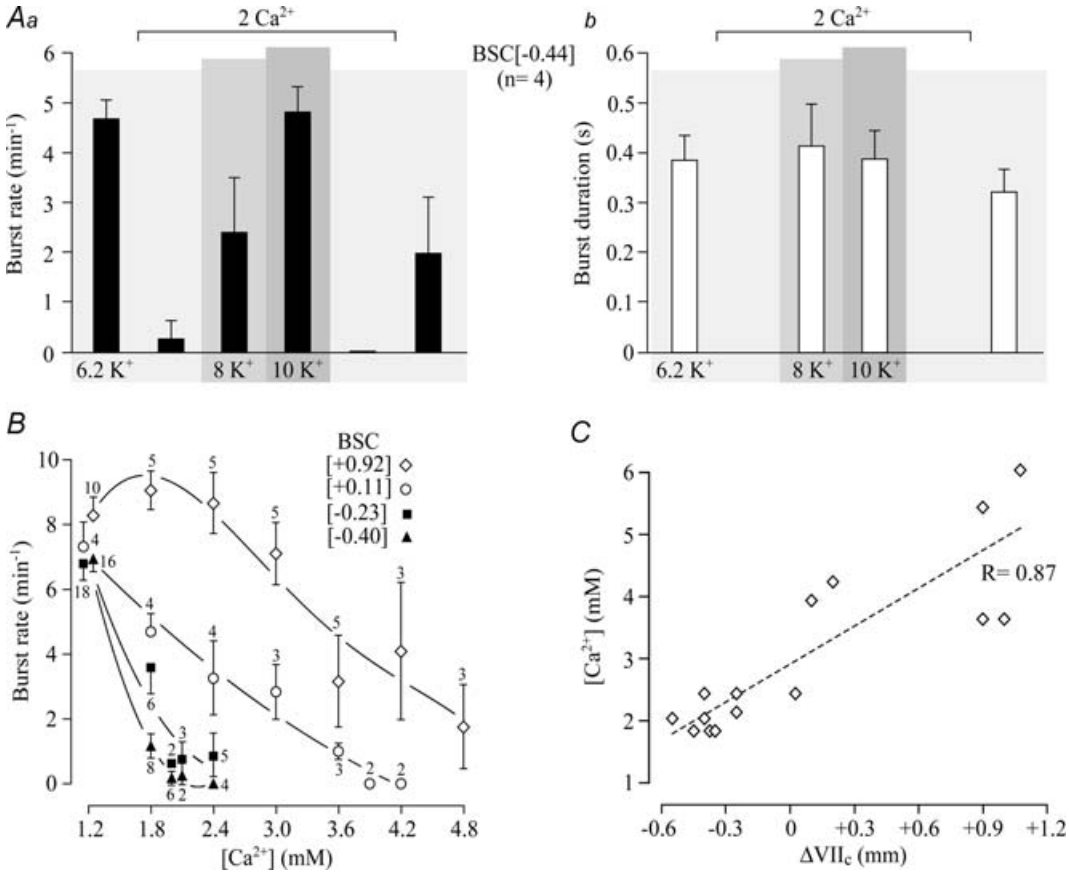

Figure 14. Dependence of Ca^{2+}-induced depression of cervical rhythm on rostral boundary in brainstem–spinal cords
A, effects of raising Ca^{2+} from 1.2 to 2 mM on mean rate (*Aa*) and duration (*Ab*) of cervical bursts in 4 BSC[−0.44] without VII. *B*, effects of increased Ca^{2+} on cervical burst rates in 4 groups of brainstem–spinal cords with different mean rostral boundaries referred to VIIc indicated in brackets, specifically $+0.92 \pm 0.15$ ($n = 10$), $+0.11 \pm 0.07$ ($n = 4$), -0.23 ± 0.07 ($n = 18$) and -0.40 ± 0.05 ($n = 16$). Note that 1.8–2 mM Ca^{2+} had a major depressing effect on rhythm in preparations without VII (filled symbols), whereas > 3 mM Ca^{2+} was necessary for a notable depression of burst rate in preparations with (portions of) VII (open symbols). Digits next to symbols indicate the number of preparations tested. *C*, significant ($P < 0.01$) relation between superfusate Ca^{2+} necessary to abolish preBötC rhythm and the rostral boundary of brainstem–spinal cords referred to their distance from VII_c (ΔVII_c). Note that considerably higher Ca^{2+} levels were necessary to block rhythm in preparations with complete VII. Values represent means and S.E.M.

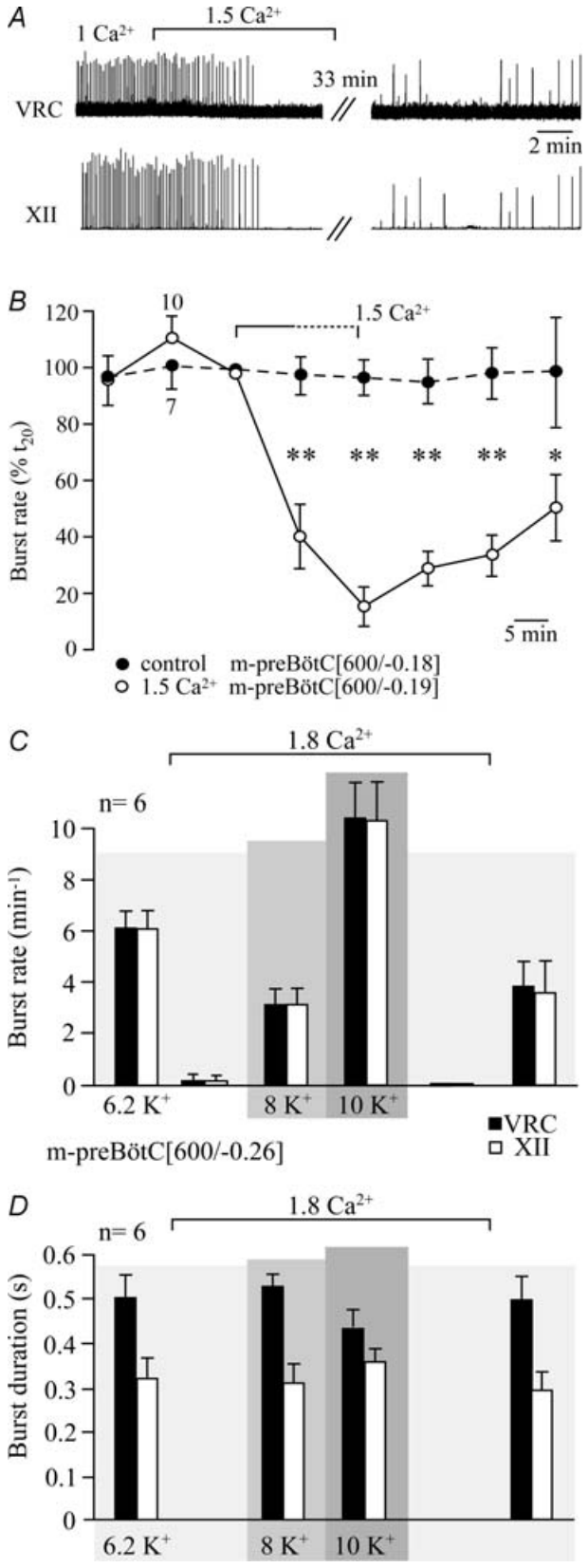

Figure 15. Block by Ca^{2+} of preBötC and XII rhythm in preBötC slices

A, synchronous inspiratory bursting of XII nerve and VRC/preBötC in a m-preBötC[600/−0.30]W-P1 slice was abolished by raising superfusate Ca^{2+} from 1 to 1.5 mM (in 3 mM K^+ and 2 mM Mg^{2+}). Note that rhythm did not fully recover within > 40 min after return to 1 mM Ca^{2+}. *B*, plot of burst rate of 10 m-preBötC[600/−0.19] slices with mean boundaries 0.19 ± 0.10/0.82 ± 0.05 mm caudal to VII_c (○) in response to 1.5 mM Ca^{2+} (in 3 mM K^+ and 2 mM Mg^{2+}). The dotted line in bracket indicating the application of elevated [Ca^{2+}] symbolizes that administration periods varied between 10 and 20 min depending on when the inhibitory effect reached steady-state. Filled circles indicate burst rates in 7 control m-preBötC[600/−0.18] slices with mean boundaries 0.18 ± 0.11/0.78 ± 0.10 mm caudal to VII_c in 1 mM Ca^{2+}, 3 mM K^+ and 2 mM Mg^{2+} solution. Asterisks show significant (*$P < 0.05$; **$P < 0.01$) difference between controls and the group treated with 1.5 mM Ca^{2+}. *C* and *D*, mean rate (*C*) and duration (*D*) of VRC/preBötC (■) and XII bursts (□) in 6 m-preBötC[600/−0.26] slices with mean boundaries 0.26 ± 0.12/0.86 ± 0.03 mm caudal to VII_c during variation of superfusate Ca^{2+} and K^+. In control, slices were kept in 6.2 mM K^+, 1 mM Ca^{2+} and 2 mM Mg^{2+}. Subsequently, rhythm was blocked upon elevation of Ca^{2+} to 1.8 mM and reactivated by raising K^+, first to 8 mM, then to 10 mM. Rhythm was blocked again upon return to 1.8 mM Ca^{2+} in 6.2 mM K^+ and recovered to values close to control following lowering of Ca^{2+} to 1 mM.

VII and those cut close to the rostral preBötC boundary. This suggests that rhythmogenic preBötC networks are not subjected to a major specific frequency modulation by rostrally neighbouring portions of the BötC or RTN/pFRG, in line with our findings in *en bloc* medullas (Smith *et al.* 1991) and, more recently, in preBötC slices (Ruangkittisakul *et al.* 2006). In extension of these studies, we show that the longevity of cervical and hypoglossal rhythms is limited to < 1.5 h, when the transection is at, or removes some portion of, the rostral preBötC. As one explanation, long-term preBötC rhythm in *en bloc* medullas may depend on drive from more rostral respiratory networks (Feldman & Janczewski, 2006; Onimaru & Homma, 2006). However, rhythm in 1.2 mM Ca^{2+} and 3 mM K^+ lasted for considerably shorter time periods in 600 μm m-preBötC slices (~1.5 h) than in *en bloc* medullas (~4 h) with similar rostral boundaries between preBötC and VII_c. This would suggest that caudal structures also drive the preBötC. But, since longevity of rhythms is greater in 600 μm compared to 500 μm m-preBötC slices (Ruangkittisakul *et al.* 2006), it is more likely that the amount of neighbouring tissue, rather than a specific rostral or caudal (respiratory) structure, determines the strength of drive to the preBötC. In that regard, one of several possible explanations for spontaneous arrest of rhythm in 3 mM K^+ is a washout of excitatory neuromodulator(s), which would occur more rapidly in preparations with exposed preBötC (Ruangkittisakul *et al.* 2006).

Sectioning at the preBötC border removes distal dendrites of preBötC neurons that extend 0.3–0.4 mm rostrocaudally (S. W. Schwarzacher & K. Ballanyi, unpublished observations). Sectioning thus reduces the connectivity and recurrent excitation within and between the bilaterally organized preBötC regions, which is

presumably pivotal for rhythm generation at physiological K^+ (Ramirez *et al.* 2002; Del Negro *et al.* 2005). This would explain why rhythm stops after shorter time periods in highly reduced *en bloc* preparations. Inspiratory rhythms were reactivated by raised K^+ or the blocker of cAMP-specific phosphodiesterase-4 rolipram. The stimulatory action of rolipram supports previous assumptions of the pivotal role of cAMP for maintaining respiratory rhythm (Ballanyi *et al.* 1997, 1999; Richter *et al.* 1997; Ruangkittisakul *et al.* 2006). In addition to the spontaneous arrest of preBötC rhythm in physiological Ca^{2+}/K^+ solution, we showed a time-dependent decrease in the duration of preBötC and cervical/hypoglossal nerve bursts. Such 'rundown' of burst duration (which was moderate for hypoglossal rhythm in *en bloc* preparations) was reversed by raised K^+ (and in most cases by rolipram) as a further indication of a proposed washout of endogenous excitatory neurostimulator(s). This phenomenon has to be taken into account for studies analysing neuromodulator effects on the strength of inspiratory activities in slice and *en bloc* models. Elevating superfusate K^+ for a stable burst duration may not be adequate as this would eventually decrease the sensitivity of preBötC networks to neuroactive agents such as opioids (Onimaru *et al.* 2006; Ruangkittisakul *et al.* 2006).

Ca^{2+}/K^+ antagonism of preBötC rhythms

One major finding of this study explains the limited longevity in physiological Ca^{2+}/K^+ of rhythms generated by the preBötC after rostral exposure (brainstem–spinal cords) or isolation (slices). In highly reduced *en bloc* medullas, raising Ca^{2+} by only 0.6 mM from 1.2 mM greatly depressed cervical and hypoglossal rhythms. This Ca^{2+} sensitivity of preBötC-driven motor systems is likely to be even higher as these preparations were kept at 6.2 mM instead of 3 mM K^+ for stabilization of rhythm, while further elevation of K^+ to 8–10 mM reversed the Ca^{2+} block. In line with that view, both the longevity and long-term burst rate of preBötC slice rhythms in 3 mM K^+ were substantially augmented in 1 mM instead 1.2 mM Ca^{2+}, whereas raising Ca^{2+} from 1 to 1.5 mM in 3 mM K^+ depressed burst rate to $< 20\%$ of control. This supports our hypothesis that raised superfusate Ca^{2+} is responsible for depressed cervical rhythms in transected brainstem–spinal cords (Onimaru & Homma, 1987; McLean & Remmers, 1994; Onimaru *et al.* 2006). First, our findings suggest that preBötC slices are not active in 2.4 mM Ca^{2+} 'Suzue-type' superfusate used by numerous groups (see Methods for references). Also, we propose that robust slice rhythm in 3 mM K^+ in our recent study (Ruangkittisakul *et al.* 2006) is, at least partly, related to use of 1 mM superfusate Ca^{2+}. As a third implication, longevity of rhythms in *en bloc* preparations with exposed preBötC will likely be substantially greater in 1 mM instead of 1.2 mM Ca^{2+}.

The finding that the Ca^{2+} block of rhythm is also revealed in preBötC recordings in the slices excludes the possibility that raised Ca^{2+} primarily affects (pre)motor circuits. The Ca^{2+} block of primary preBötC rhythm can, nevertheless, be indirect as suggested by the finding that block of slice rhythm by bath-application of persistent Na^+ channel blockers is mimicked by local injection of the agents into the raphe, but not the preBötC (Pace *et al.* 2007). Performing a similar test was beyond the scope of this study, as was to elaborate the mechanism of Ca^{2+} block. As one possibility, Ca^{2+} may inhibit preBötC cells or tonic neurons driving the preBötC via a more pronounced stimulatory effect on (tonic) inhibitory than on excitatory synapses (Jefferys, 1995). In fact, $GABA_A$ and glycine receptors depress inspiratory bursting in newborn rat brainstem–spinal cords (Onimaru *et al.* 1990; Brockhaus & Ballanyi, 1998, 2000). Ca^{2+}-induced block of rhythm could also be caused by Ca^{2+} screening of negative membrane surface charges (Hille, 2001; Somjen, 2002). However, if this was the main mechanism, raising Mg^{2+} from 1 to 2 mM should have a similar blocking effect on slice rhythms, while returning to normal Ca^{2+} should have reversed the depression. Alternatively, raised Ca^{2+} may have long-term effects on Ca^{2+} homeostasis in respiratory (drive) neurons with low Ca^{2+} buffering capacity (Alheid *et al.* 2002).

In line with our findings, early *in vivo* studies showed that Ca^{2+} injection into the ventriculo-cisternal space depresses breathing (Berndt *et al.* 1969; Leusen, 1972; Berkenbosch & Adan, 1974). In that regard, a Ca^{2+}/K^+ antagonism was proposed to compensate for respiratory depression by Ca^{2+} when K^+ was simultaneously injected (Leusen, 1972). Moreover, our results show that isolated preBötC rhythms at physiological K^+ are stimulated by decreasing superfusate Ca^{2+}. We chose 1.2 mM for our standard solution as a major number of *in vivo* studies reported values of 1.1–1.3 mM for interstitial Ca^{2+} in diverse brain tissue, including the ventral respiratory column (Heinemann *et al.* 1977; Nicholson *et al.* 1978; Richter & Acker, 1989; Trippenbach *et al.* 1990; Nilsson *et al.* 1993; Puka-Sundvall *et al.* 1994; Somjen, 2002). Respiratory rhythm was also revealed in 0.8 mM Ca^{2+} and 6.2 mM K^+ superfusate in $\sim$1 mm thick mouse brainstem slices (Rekling *et al.* 1996), while hypothalamic slices generate *in vivo*-like spontaneous activity in 0.75 mM, but not > 1 mM Ca^{2+} (Pittman *et al.* 1981). Accordingly, 'real' *in vivo* extracellular Ca^{2+} levels may be close to, or slightly less than, 1 mM. However, there may be a critical minimal Ca^{2+} level as ≤ 0.5 mM superfusate Ca^{2+} is a common epilepsy model (Konnerth *et al.* 1986; Jefferys, 1995). We propose that 1 mM Ca^{2+} is best suited to study isolated preBötC functions in 3 mM K^+.

Relation of hypoglossal bursting with cervical and preBötC rhythms

Simultaneous recordings revealed 1 : 1-coupling of hypoglossal bursting with either cervical nerve activity (in *en bloc* medullas) or preBötC population activity (in slices). This argues against concerns that hypoglossal recordings may not necessarily be indicative of respiratory activity *in vitro*, in particular at hypothermia (St-John *et al.* 2004). However, the amplitude of hypoglossal bursts fluctuated periodically in 3 mM K^+, 1 mM Ca^{2+} and 1–2 mM Mg^{2+} in some slices. Elevating K^+ to 6.2–9 mM stabilized, and sometimes increased, the amplitude of hypoglossal (and preBötC) bursts and restored their durations to, or even beyond, the values during the initial phase of recordings. In contrast to a stable hypoglossal rhythm in the slices and (in rostral roots of) *en bloc* preparations transected close to or into the preBötC, rhythm was greatly depressed in all hypoglossal roots within ∼1 h in preparations containing (portions of) VII (for reasons, see below). This finding is important for studies devoted to the analysis of the function of hypoglossal neurons in *en bloc* medullas. For example, it was proposed that serotonin depresses hypoglossal, but not phrenic, motor output in brainstem–spinal cords (Monteau *et al.* 1990). In such studies, it is pivotal to test first for stable control hypoglossal nerve amplitudes.

Influence of restricted diffusion on respiratory activities in *en bloc* medullas

Notably higher superfusate Ca^{2+} levels were necessary to block rhythm in less-reduced *en bloc* preparations, e.g. $\geq$ 3.6 mM in brainstems with complete VII. This is in line with the observation that 4 mM Ca^{2+} depressed cervical bursting in such preparations (Kuwana *et al.* 1998). As one explanation for this phenomenon, (respiratory) structures in the rostral medulla may be less sensitive to Ca^{2+}, thus being capable of driving the preBötC in high Ca^{2+}. Alternatively, the decreased Ca^{2+} sensitivity of inspiratory rhythms may result from the larger dimension of *en bloc* preparations, constituting a diffusion barrier for build-up, e.g. of a modest interstitial K^+ gradient (and a pH gradient) by an anoxic core that does not, however, appear to contain pivotal O_2- or pH-sensitive inspiratory structures (Ballanyi *et al.* 1992, 1999; Brockhaus *et al.* 1993; Ballanyi, 2004). It may, though, be argued that the pre/postinspiratory activity pattern of newborn rat pFRG neurons *in vitro* results from hypoxia/anoxia in *en bloc* preparations with more rostral tissue as evoked hypoxia activated preinspiratory bursting in postinspiratory ventral respiratory column neurons of adult rats (Schwarzacher *et al.* 1991). It may further be speculated that transection 0.6 mm or less rostral to VII_c reduces the anoxic core, inactivates these neurons and, consequently, silences lumbar pre/postinspiratory bursting. However, several findings argue against this hypothetical scenario. First, preinspiratory activity was also induced in postinspiratory neurons of the latter *in vivo* study by prolonged lung inflation or deflation during normoxia. Second, pre/postinspiratory abdominal muscle activity is seen in normoxic juvenile rats *in vivo* (Janczewski & Feldman, 2006). Furthermore, experimentally induced anoxia blocks the preinspiratory and greatly augments the postinspiratory component of pFRG-related activities (Ballanyi, 2004), opposite to the above *in vivo* findings by Schwarzacher *et al.* (1991). Finally, rostral pFRG neurons are located within $< 300\ \mu$m from the ventral brainstem surface (Onimaru & Homma, 2003), whereas the anoxic core is restricted to tissue depths $> 700\ \mu$m (Brockhaus *et al.* 1993).

In preparations with a major amount of rostral tissue, extracellular $[K^+]$ is several millimolar higher in the vicinity of preBötC neurons than in the superfusate, due to the modest K^+ gradient (Brockhaus *et al.* 1993; Okada *et al.* 2005). These elevated interstitial K^+ levels may antagonize the depressing action of elevated superfusate Ca^{2+} as suggested by the finding that preBötC rhythm persisted in 'Suzue-type' solution after transection of brainstem–spinal cords between the preBötC and VII, but was abolished upon subsequent removal of the transected rostral aspect of the preparation (Onimaru *et al.* 2006). Consequently, lower K^+ (e.g. 2 mM), may be used instead of 3 mM in *en bloc* preparations with more rostral tissue to compensate for changes in the interstitial Ca^{2+}/K^+ ratio. Hampered diffusion of raised Ca^{2+} into the tissue could also explain the attenuated blocking effect. However, this is not likely as millimolar superfusate Ca^{2+} concentrations equilibrate within minutes in this *en bloc* preparation, which does not show an interstitial Ca^{2+} gradient in control (Völker *et al.* 1995; Ballanyi *et al.* 1996; Kuwana *et al.* 1998). Also the longevity of hypoglossal rhythms depended on the rostrocaudal extension of *en bloc* medullas. We hypothesize that arrest of hypoglossal bursting in preparations with VII is caused by accumulation of inhibitory neuromodulator(s) and/or metabolite(s) depressing hypoglossal (pre)motoneurons, but not preBötC interneurons and cervical premotoneurons.

Conclusions

The isolated inspiratory centre generates robust rhythm in physiological cation solution. preBötC rhythms are blocked by minor extracellular Ca^{2+} rises, but can be restored by additional notable elevation of extracellular K^+. The dependence of inspiratory-related rhythms on this strong Ca^{2+}/K^+ antagonism decreases in *en bloc* preparations with increasing amount of tissue rostral to

the preBötC. Based on these findings, we recommend the use of superfusate Ca^{2+} levels at the lower end of the physiological spectrum, i.e. 1 mM, for the study of functions of the isolated preBötC in physiological K^+. In addition, one may consider the use of reduced superfusate K^+ (e.g. 2 mM) for studies of respiratory rhythms in *en bloc* preparations with extended rostral tissue. It should be considered further that hypoglossal rhythm is blocked in such less-reduced brainstem–spinal cords, whereas pre/postinspiratory lumbar bursting is absent in more reduced *en bloc* medullas. Our findings suggest that discrepant results using *en bloc* preparations with varying rostral boundaries may be partly explained by different dimensions, affecting diffusion of endogenous neuromodulators, rather than changes in specific structures present in more rostral respiratory regions. We hypothesize that the preBötC is more sensitive in such solutions to CO_2/H^+, hypoxia/anoxia or neuromodulators such as (endogenous) opiates or substance P, all of which determine respiratory rhythm *in vivo*.

References

Alheid GF, Gray PA, Jiang MC, Feldman JL & McCrimmon DR (2002). Parvalbumin in respiratory neurons of the ventrolateral medulla of the adult rat. *J Neurocytol* **31**, 693–717.

Alheid GF, Milsom WK & McCrimmon DR (2004). Pontine influences on breathing: an overview. *Respir Physiol Neurobiol* **143**, 105–114.

Arata A, Onimaru H & Homma I (1990). Respiration-related neurons in the ventral medulla of newborn rats in vitro. *Brain Res Bull* **24**, 599–604.

Ballanyi K (1999). Isolated tissues. In vitro preparations. In *Modern Techniques in Neuroscience Research*, ed. Windhorst U & Johansson H, pp. 307–326. Springer, Heidelberg.

Ballanyi K (2004). Neuromodulation of the perinatal respiratory network. *Curr Neuropharmacol* **2**, 221–243.

Ballanyi K, Kuwana S, Völker A, Morawietz G & Richter DW (1992). Developmental changes in the hypoxia tolerance of the in vitro respiratory network of rats. *Neurosci Lett* **148**, 141–144.

Ballanyi K, Lalley PM, Hoch B & Richter DW (1997). cAMP-dependent reversal of opioid- and prostaglandin-mediated depression of the isolated respiratory network in newborn rats. *J Physiol* **504**, 127–134.

Ballanyi K, Onimaru H & Homma I (1999). Respiratory network function in the isolated brainstem-spinal cord of newborn rats. *Progr Neurobiol* **59**, 583–634.

Ballanyi K, Völker A & Richter DW (1996). Functional relevance of anaerobic metabolism in the isolated respiratory network of newborn rats. *Pflugers Arch* **432**, 741–748.

Berkenbosch A & Adan AJ (1974). Influence of CSF calcium concentration on the ventilatory response to CO_2 and O_2. *Pflugers Arch* **348**, 33–50.

Berndt J, Fenner A & Berger K (1969). Influence of calcium and magnesium on the respiratory response to changes in CSF pH. *Respir Physiol* **7**, 216–229.

Brockhaus J & Ballanyi K (1998). Synaptic inhibition in the isolated respiratory network of neonatal rats. *Eur J Neurosci* **10**, 3823–3839.

Brockhaus J & Ballanyi K (2000). Anticonvulsant adenosine A_1 receptor-mediated adenosine action on neuronal networks in the brainstem-spinal cord of newborn rats. *Neuroscience* **96**, 359–371.

Brockhaus J, Ballanyi K, Smith JC & Richter DW (1993). Microenvironment of respiratory neurons in the *in vitro* brainstem-spinal cord of neonatal rats. *J Physiol* **462**, 421–445.

Brown PD, Davies SL, Speake T & Millar ID (2004). Molecular mechanisms of cerebrospinal fluid production. *Neuroscience* **129**, 957–970.

De Araujo AC & Campos R (2005). A systematic study of the brain base arteries and their blood supply sources in the chinchilla (*Chinchilla lanigeria* – Molina 1782). *Braz J Morph Sci* **22**, 221–232.

Del Negro CA, Morgado-Valle C, Hayes JA, Mackay DD, Pace RW, Crowder EA & Feldman JL (2005). Sodium and calcium current-mediated pacemaker neurons and respiratory rhythm generation. *J Neurosci* **25**, 446–453.

Errchidi S, Monteau R & Hilaire G (1991). Noradrenergic modulation of the medullary respiratory rhythm generator in the newborn rat: an in vitro study. *J Physiol* **443**, 477–498.

Feldman JL (1986). Neurophysiology of breathing in mammals. In *Handbook of Physiology*, section 1, *The Nervous System*, vol. IV, *Intrinsic Regulatory Systems in the Brain*, Chap 9. Ed, Mountcastle VB, pp. 463–524. American Physiological Society, Bethesda.

Feldman JL & Del Negro CA (2006). Looking for inspiration: new perspectives on respiratory rhythm. *Nat Rev Neurosci* **7**, 232–242.

Feldman JL & Janczewski WA (2006). Point : Counterpoint: The parafacial respiratory group (pFRG)/pre-Botzinger complex (preBotC) is the primary site of respiratory rhythm generation in the mammal. Counterpoint: the preBotC is the primary site of respiratory rhythm generation in the mammal. *J Appl Physiol* **100**, 2096–2097; Discussion 2097–2098, 2103–2108.

Hansen AJ (1985). Effect of anoxia on ion distribution in the brain. *Physiol Rev* **65**, 101–148.

Heinemann U, Lux HD & Gutnick MJ (1977). Extracellular free calcium and potassium during paroxsmal activity in the cerebral cortex of the cat. *Exp Brain Res* **27**, 237–243.

Herlenius E, Aden U, Tang LQ & Lagercrantz H (2002). Perinatal respiratory control and its modulation by adenosine and caffeine in the rat. *Pediatr Res* **51**, 4–12.

Hille B (2001). *Ion Channels of Excitable Membranes*. Sinauer Associates, Sunderland, MA, USA.

Iizuka M (2004). Rostrocaudal distribution of spinal respiratory motor activity in an in vitro neonatal rat preparation. *Neurosci Res* **50**, 263–269.

Janczewski WA & Feldman JL (2006). Distinct rhythm generators for inspiration and expiration in the juvenile rat. *J Physiol* **570**, 407–420.

Janczewski WA, Onimaru H, Homma I & Feldman JL (2002). Opioid-resistant respiratory pathway from the preinspiratory neurones to abdominal muscles: in vivo and in vitro study in the newborn rat. *J Physiol* **545**, 1017–1026.

Jefferys JG (1995). Nonsynaptic modulation of neuronal activity in the brain: electric currents and extracellular ions. *Physiol Rev* **75**, 689–723.

Johnson SM, Smith JC & Feldman JL (1996). Modulation of respiratory rhythm in vitro: role of $G_{i/o}$ protein-mediated mechanisms. *J Appl Physiol* **80**, 2120–2133.

Konnerth A, Heinemann U & Yaari Y (1986). Nonsynaptic epileptogenesis in the mammalian hippocampus in vitro. I. Development of seizurelike activity in low extracellular calcium. *J Neurophysiol* **56**, 409–423.

Koshiya N & Smith JC (1999). Neuronal pacemaker for breathing visualized in vitro. *Nature* **400**, 360–363.

Kuwana S, Okada Y & Natsui T (1998). Effects of extracellular calcium and magnesium on central respiratory control in the brainstem-spinal cord of neonatal rat. *Brain Res* **786**, 194–204.

Kuwana S, Tsunekawa N, Yanagawa Y, Okada Y, Kuribayashi J & Obata K (2006). Electrophysiological and morphological characteristics of GABAergic respiratory neurons in the mouse pre-Botzinger complex. *Eur J Neurosci* **23**, 667–674.

Leusen I (1972). Regulation of cerebrospinal fluid composition with reference to breathing. *Physiol Rev* **52**, 1–56.

McLean HA & Remmers JE (1994). Respiratory motor output of the sectioned medulla of the neonatal rat. *Respir Physiol* **96**, 49–60.

Mellen NM, Janczewski WA, Bocchiaro CM & Feldman JL (2003). Opioid-induced quantal slowing reveals dual networks for respiratory rhythm generation. *Neuron* **37**, 821–826.

Monnier A, Alheid GF & McCrimmon DR (2003). Defining ventral medullary respiratory compartments with a glutamate receptor agonist in the rat. *J Physiol* **548**, 859–874.

Monteau R, Errchidi S, Gauthier P, Hilaire G & Rega P (1989). Pneumotaxic centre and apneustic breathing: interspecies differences between rat and cat. *Neurosci Lett* **99**, 311–316.

Monteau R, Morin D, Hennequin S & Hilaire G (1990). Differential effects of serotonin on respiratory activity of hypoglossal and cervical motoneurons: an in vitro study on the newborn rat. *Neurosci Lett* **111**, 127–132.

Nicholson C, ten Bruggencate G, Stockle H & Steinberg R (1978). Calcium and potassium changes in extracellular microenvironment of cat cerebellar cortex. *J Neurophysiol* **41**, 1026–1039.

Nilsson P, Hillered L, Olsson Y, Sheardown MJ & Hansen AJ (1993). Regional changes in interstitial K^{+} and Ca^{2+} levels following cortical compression contusion trauma in rats. *J Cereb Blood Flow Metab* **13**, 183–192.

O'Donnell JM & Zhang HT (2004). Antidepressant effects of inhibitors of cAMP phosphodiesterase (PDE4). *Trends Pharmacol Sci* **25**, 158–163.

Okada Y, Kuwana S, Kawai A, Muckenhoff K & Scheid P (2005). Significance of extracellular potassium in central respiratory control studied in the isolated brainstem-spinal cord preparation of the neonatal rat. *Respir Physiol Neurobiol* **146**, 21–32.

Onimaru H, Arata A & Homma I (1990). Inhibitory synaptic inputs to the respiratory rhythm generator in the medulla isolated from newborn rats. *Pflugers Arch* **417**, 425–432.

Onimaru H, Ballanyi K & Homma I (2003). Contribution of Ca^{2+}-dependent conductances to membrane potential fluctuations of medullary respiratory neurons of newborn rats in vitro. *J Physiol* **552**, 727–741.

Onimaru H & Homma I (1987). Respiratory rhythm generator neurons in medulla of brainstem-spinal cord preparation from newborn rat. *Brain Res* **403**, 380–384.

Onimaru H & Homma I (2003). A novel functional neuron group for respiratory rhythm generation in the ventral medulla. *J Neurosci* **23**, 1478–1486.

Onimaru H & Homma I (2006). Point : Counterpoint: The parafacial respiratory group (pFRG)/pre-Botzinger complex (preBotC) is the primary site of respiratory rhythm generation in the mammal. Point: The pFRG is the primary site of respiratory rhythm generation in the mammal. *J Appl Physiol* **100**, 2094–2095; Discussion 2097–2098, 2103–2108.

Onimaru H, Kumagawa Y & Homma I (2006). Respiration-related rhythmic activity in the rostral medulla of newborn rats. *J Neurophysiol* **96**, 55–61.

Oshima N, Kumagai H, Kawai A, Sakata K, Matsuura T & Saruta T (2000). Three types of putative presympathetic neurons in the rostral ventrolateral medulla studied with rat brainstem-spinal cord preparation. *Auton Neurosci* **84**, 40–49.

Pace RW, Mackay DD, Feldman JL & Del Negro CA (2007). Role of persistent sodium current in mouse preBotzinger complex neurons and respiratory rhythm generation. *J Physiol* **580**, 485–496.

Paton JF, Abdala AP, Koizumi H, Smith JC & St-John WM (2006). Respiratory rhythm generation during gasping depends on persistent sodium current. *Nat Neurosci* **9**, 311–313.

Pittman QJ, Hatton JD & Bloom FE (1981). Spontaneous activity in perfused hypothalamic slices: dependence on calcium content of perfusate. *Exp Brain Res* **42**, 49–52.

Puka-Sundvall M, Hagberg H & Andine P (1994). Changes in extracellular calcium concentration in the immature rat cerebral cortex during anoxia are not influenced by MK-801. *Brain Res Dev Brain Res* **77**, 146–150.

Ramirez JM, Zuperku EJ, Alheid GF, Lieske SP, Ptak K & McCrimmon DR (2002). Respiratory rhythm generation: converging concepts from in vitro and in vivo approaches? *Respir Physiol Neurobiol* **131**, 43–56.

Rekling JC, Champagnat J & Denavit-Saubie M (1996). Electroresponsive properties and membrane potential trajectories of three types of inspiratory neurons in the newborn mouse brain stem in vitro. *J Neurophysiol* **75**, 795–810.

Richter DW & Acker H (1989). Respiratory neuron behaviour during medullary hypoxia. In *Chemoreceptors and Reflexes in Breathing: Cellular and Molecular Aspects*, ed. Lahiri S, pp. 267–274. Oxford University Press, Oxford.

Richter DW, Lalley PM, Pierrefiche O, Haji A, Bischoff AM, Wilken B & Hanefeld V (1997). Intracellular signal pathways controlling respiratory neurons. *Respir Physiol* **110**, 113–123.

Ruangkittisakul A & Ballanyi K (2006). Reversal by phosphodiesterase-4 blockers of in vitro apnea in the isolated brainstem-spinal cord preparation from newborn rats. *Neurosci Lett* **401**, 194–198.

Ruangkittisakul A, Schwarzacher SW, Ma Y, Poon B, Secchia L, Funk GD & Ballanyi K (2006). High sensitivity to neuromodulator-activated signalling pathways at physiological [K^+] of confocally-imaged respiratory centre neurons in online-calibrated newborn rat brainstem slices. *J Neurosci* **26**, 11870–11880.

Schwarzacher SW, Smith JC & Richter DW (1995). Pre-Bötzinger complex in the cat. *J Neurophysiol* **73**, 1452–1461.

Schwarzacher SW, Wilhelm Z, Anders K & Richter DW (1991). The medullary respiratory network in the rat. *J Physiol* **435**, 631–644.

Smith JC, Ellenberger HH, Ballanyi K, Richter DW & Feldman JL (1991). Pre-Bötzinger complex: a brainstem region that may generate respiratory rhythm in mammals. *Science* **254**, 726–729.

Smith JC, Greer JJ, Liu GS & Feldman JL (1990). Neural mechanisms generating respiratory pattern in mammalian brain stem-spinal cord in vitro. I. Spatiotemporal patterns of motor and medullary neuron activity. *J Neurophysiol* **64**, 1149–1169.

Somjen GG (2002). Ion regulation in the brain: implications for pathophysiology. *Neuroscientist* **8**, 254–267.

St-John WM, Paton JF & Leiter JC (2004). Uncoupling of rhythmic hypoglossal from phrenic activity in the rat. *Exp Physiol* **89**, 727–737.

St-John WM, Rudkin AH, Harris MR, Leiter JC & Paton JF (2005). Maintenance of eupnea and gasping following alterations in potassium ion concentration of perfusates of in situ rat preparation. *J Neurosci Methods* **142**, 125–129.

Sun QJ, Goodchild AK, Chalmers JP & Pilowsky PM (1998). The pre-Botzinger complex and phase-spanning neurons in the adult rat. *Brain Res* **809**, 204–213.

Suzue T (1984). Respiratory rhythm generation in the in vitro brain stem-spinal cord preparation of the neonatal rat. *J Physiol* **354**, 173–183.

Trippenbach T, Richter DW & Acker H (1990). Hypoxia and ion activities within the brain stem of newborn rabbits. *J Appl Physiol* **68**, 2494–2503.

Völker A, Ballanyi K & Richter DW (1995). Anoxic disturbance of the isolated respiratory network of neonatal rats. *Exp Brain Res* **103**, 9–19.

Wilson RJ, Vasilakos K & Remmers JE (2006). Phylogeny of vertebrate respiratory rhythm generators: the oscillator homology hypothesis. *Respir Physiol Neurobiol* **154**, 47–60.

Acknowledgements

This work was supported by the Canadian Institutes of Health Research (CIHR), the Canadian Foundation for Innovation (CFI) and the Alberta Heritage Foundation for Medical Research (AHFMR). K.B. is an AHFMR Scientist. A.R. has been awarded a CIHR studentship (MFN training grant). We thank Dr G. F. Alheid for critical comments on the histological sections of the manuscript.

Supplemental material

Online supplemental material for this paper can be accessed at:
http://jp.physoc.org/cgi/content/full/jphysiol.2007.142760/DC1
and
http://www.blackwell-synergy.com/doi/suppl/10.1113/jphysiol.2007.142760